Requirement of Interaction between Mast Cells and Skin Dendritic Cells to Establish Contact Hypersensitivity

Atsushi Otsuka[1,2], Masato Kubo[3], Tetsuya Honda[1], Gyohei Egawa[1], Saeko Nakajima[1], Hideaki Tanizaki[1], Bongju Kim[2], Satoshi Matsuoka[2], Takeshi Watanabe[2], Susumu Nakae[4], Yoshiki Miyachi[1], Kenji Kabashima[1]*

1 Department of Dermatology, Kyoto University Graduate School of Medicine, Kyoto, Japan, **2** Center for Innovation in Immunoregulative Technology and Therapeutics, Kyoto University Graduate School of Medicine, Kyoto, Japan, **3** Laboratory for Signal Network, Research Center for Allergy and Immunology, RIKEN Yokohama Institute, Tsurumi, Yokohama, Kanagawa, Japan, **4** Frontier Research Initiative, Institute of Medical Science, University of Tokyo, Minato, Tokyo, Japan

Abstract

The role of mast cells (MCs) in contact hypersensitivity (CHS) remains controversial. This is due in part to the use of the MC-deficient *Kit*$^{W/Wv}$ mouse model, since *Kit*$^{W/Wv}$ mice congenitally lack other types of cells as a result of a point mutation in c-kit. A recent study indicated that the intronic enhancer (IE) for *Il4* gene transcription is essential for MCs but not in other cell types. The aim of this study is to re-evaluate the roles of MCs in CHS using mice in which MCs can be conditionally and specifically depleted. Transgenic Mas-TRECK mice in which MCs are depleted conditionally were newly generated using cell-type specific gene regulation by IE. Using this mouse, CHS and FITC-induced cutaneous DC migration were analyzed. Chemotaxis assay and cytoplasmic Ca^{2+} imaging were performed by co-culture of bone marrow-derived MCs (BMMCs) and bone marrow-derived dendritic cells (BMDCs). In Mas-TRECK mice, CHS was attenuated when MCs were depleted during the sensitization phase. In addition, both maturation and migration of skin DCs were abrogated by MC depletion. Consistently, BMMCs enhanced maturation and chemotaxis of BMDC in ICAM-1 and TNF-α dependent manners Furthermore, stimulated BMDCs increased intracellular Ca^{2+} of MC upon direct interaction and up-regulated membrane-bound TNF-α on BMMCs. These results suggest that MCs enhance DC functions by interacting with DCs in the skin to establish the sensitization phase of CHS.

Citation: Otsuka A, Kubo M, Honda T, Egawa G, Nakajima S, et al. (2011) Requirement of Interaction between Mast Cells and Skin Dendritic Cells to Establish Contact Hypersensitivity. PLoS ONE 6(9): e25538. doi:10.1371/journal.pone.0025538

Editor: Nirbhay Kumar, Tulane University, United States of America

Received May 12, 2011; **Accepted** September 6, 2011; **Published** September 30, 2011

Funding: This work was supported in part by Grants-in-Aid for Scientific Research from the Ministry of Education, Culture, Sports, Science and Technology of Japan. The funders had no role in study design, data collection and analysis, decision to publish, or preparation of the manuscript. No additional external funding received for this study.

Competing Interests: The authors have declared that no competing interests exist.

* E-mail: kaba@kuhp.kyoto-u.ac.jp

Introduction

Contact hypersensitivity (CHS) has been widely used to study cutaneous immune responses, since it is a prototype of delayed-type hypersensitivity mediated by antigen -specific T cells [1,2,3,4]. An essential step in the sensitization phase for CHS is the migration of hapten-bearing cutaneous dendritic cells (DCs), such as epidermal Langerhans cells (LCs) and dermal DCs, into skin-draining lymph nodes (LNs). After completing their maturation, mature DCs present antigen to naive T cells in the LNs, thus establishing the sensitization phase. In the subsequent challenge phase, re-exposure to the cognate hapten results in the recruitment of antigen-specific T cells and other non-antigen-specific leukocytes.

The functions of cutaneous DCs are modulated by keratinocyte-derived proinflammatory cytokines [1,5]. The role of the different skin DC subsets in CHS (inducers, regulators, or functional redundancy) is a matter of active debate [6]. In addition, dermal DCs, including Langerin (CD207)$^+$ dermal DCs, may also play an important role in CHS [7,8].

Mast cells (MCs) are a candidate DC modulator since they express and release a wide variety of intermediaries, such as histamine, tumor necrosis factor (TNF)-α and lipid mediators. It has been reported that activated human cord blood-derived MCs induce DC maturation *in vitro* [9], that IgE-stimulated MC-derived histamine induces murine LC migration *in vivo* [10], and that MC-derived TNF-α promotes cutaneous murine DC migration *in vivo* in an IgE-independent manner [11]. On the other hand, prostaglandin (PG) D_2 produced by MCs in response to allergens [12], inhibits LC migration [13]. Therefore, MCs might have bi-directional effects on DC activity in a context-dependent manner and the question of the mechanisms by which DCs are modulated by MCs is an important issue to pursue.

While MCs have been assumed to play an important role in CHS, their role is controversial. Previous studies have demonstrated that MC-deficient *Kit*$^{W/Wv}$ mice show attenuated CHS responses, meanwhile, other studies have shown that CHS was not impaired in *Kit*$^{W/Wv}$ mice [14]. Although some studies indicated that the discrepancy in *W/Wv* mice might be due to the difference in hapten dose, the detailed mechanism is still unclear. *Kit*$^{W/Wv}$ mice and *Kit*$^{W\text{-}sh/W\text{-}sh}$ mice have an inversion mutation in the Kit gene [15], and therefore, these mice also lack melanocytes and hematopoietic stem cells, which are known to modulate immune responses [16,17]. In addition, since MCs are congenitally absent, it is possible that compensatory mechanisms may exist that

modulates immune system functions. Therefore, it is important to re-evaluate the roles of MCs using mice in which MCs can be conditionally and specifically depleted.

Recently, we have demonstrated that MCs and basophils use specific enhancer elements, intronic enhancer (IE) and a 3′ 4kb fragment that contains 3′UTR and HS4 elements, to regulate *Il4* gene expression, respectively [18]. Taking advantage of this system, we have generated mice that contain human diphtheria toxin receptor (DTR) under the control of IE. Therefore, mast cell-specific enhancer-mediated Toxin Receptor-mediated Conditional cell Knock out (TRECK) systems were designated as Mas-TRECK transgenic (Tg) mice. In these mice, both MCs and basophils are conditionally depleted by diphtheria toxin (DT) treatment. Since basophils recover much faster than MCs (Fig S1A, B), there exist a period of specific MC depletion. Taking advantage of the system, we have herein demonstrated that activated DCs induce MC activation, which triggers the migration and maturation of DCs via cell-cell contact. This DC-MC interaction plays an essential role in the sensitization phase of CHS.

Results

Suppression of CHS responses in Mas-TRECK Tg mice

Mice expressing the human DTR under the control of IE element (for Mas-TRECK) and 3′UTR element (for basophil-specific enhancer-mediated TRECK systems; Bas-TRECK) in the *Il4* gene locus were generated by a transgenic strategy (Sawaguchi et al. Manuscript in submission). We initially demonstrated that skin MCs were completely depleted in Mas-TRECK Tg mice 5 and 12 days after an intraperitoneal injection of diphtheria toxin (DT) (See **Fig. S1A** in the Online Repository). Although DX5+ FcεRIα+ basophils in the blood were eliminated 5 days after DT treatment in Mas-TRECK Tg mice, basophil numbers recovered in 12 days (**Fig. S1B** in the Online Repository).

To investigate the role of MCs in cutaneous acquired immune responses, we used DNFB-induced CHS as a model. CHS responses were similar between wild type (WT) and Mas-TRECK Tg mice in the absence of DT treatment (205 μm±10.5 vs 212 μm±12.3; average ± SD). In addition, DT treatment itself did not affect the degree of CHS responses in WT mice. On the other hand, when both WT and Mas-TRECK Tg mice were treated with DT and assayed 12 days later, the CHS response in Mas-TRECK Tg mice was much less than that in WT mice (**Fig. 1A**). The ear swelling of WT and Mas TRECK Tg mice was 48.2 (±5.2, SD) μm and 51.3 (±4.8, SD) μ after 72 h, and 15 (±7.29, SD) μm and 40.1 (±6.68, SD) μm after 96 h respectively. Histology of the ears 48 h after the challenge showed considerable lymphocyte infiltration and edema in the dermis of sensitized WT mice; these changes were less apparent in Mas-TRECK Tg mice (**Fig. 1B, *left panel***) and the histological scores [19] in Mas-TRECK Tg mice were lower than those in WT mice (**Fig. 1B, *right panel***). On the other hand, the CHS response was not impaired in ***Kit*$^{W/Wv}$** mice (See **Fig. S2A** in the Online Repository).

In addition, the CHS response in Bas-TRECK Tg mice, which lack only basophils upon treatment with DT, was similar to that of WT mice (See **Fig. S2B** in the Online Repository). The attenuated CHS response in Mas-TRECK Tg mice was confirmed using an additional hapten, oxazolone (**Fig. 1C**) and also at higher hapten doses (See **Fig. S2C** in the Online Repository).

To clarify the action phase of MCs in CHS, we used an adoptive transfer-induced CHS model. Recipients of LN cells from sensitized WT mice showed an enhanced CHS response, whereas the recipients of LN cells from sensitized Mas-TRECK Tg mice showed a markedly inhibited response (**Fig. 1D**). In addition, the recipients of CD90.2+ T cells from sensitized Mas-TRECK Tg mice showed inhibited responses compared to recipients of CD90.2+ T cells from sensitized WT mice (See **Fig. S2D** in the Online Repository). These data indicate that MCs play important roles in establishing CHS during the sensitization phase.

We further evaluated whether the attenuated CHS in Mas-TRECK Tg mice reflected the lack of MCs. WT or Mas-TRECK Tg mice were engrafted in the skin with or without BMMCs 5×10^6 cells in 100 μl/dorsal skin 1 hour before oxazolone sensitization. The numbers of toluidine blue positive mast cells (per field) in the dermis are 40.2 (±5.3, SD) in Mas TRECK Tg mice and 35.3 (±7.2, SD) in B6 wild type mice after one hour injection of BMMC (n = 3) (See **Fig. S2E** in the Online Repository). On the other hand, the number of MCs in the uninjected sites was 10.5 (±3.2, SD) in B6 wild type mice. Five days after sensitization, the skin-draining LN cells of sensitized mice were adoptively transferred intravenously into naive WT recipients and challenged with oxazolone on the ears. The CHS response of recipients of LN cells from sensitized WT mice was not changed by the pre-engraftment of BMMCs into the skin (**Fig. 1E**). On the other hand, the attenuated CHS response of recipients of Mas-TRECK Tg LN cells was fully restored by the pre-engraftment of BMMCs into the skin.

Next we counted the cells infiltrating the skin of WT and Mas-TRECK Tg mice 12 h after challenge with DNFB. The numbers of CD45+ CD3+ CD4+ T cells, CD45+ CD3+ CD8+ T cells, and CD45+ Gr-1high neutrophils after both sensitization and challenge, and that of neutrophils after only challenge were increased in WT mice. But such increment was attenuated in Mas-TRECK Tg mice (See **Fig. S3A** in the Online Repository). Consistent with this result, the mRNA levels of IFN-γ, IL-17 and IL-1β in the skin 12 h after challenge were significantly decreased in Mas-TRECK Tg mice compared to WT mice (See **Fig. S3B** in the Online Repository).

We further analyzed the composition of LN cells after sensitization. Five days after sensitization, the skin-draining LN cells of WT and Mas-TRECK Tg mice were collected. The numbers of CD44+ CD62L+ central memory T cells and CD44+ CD62L- effector memory T cells among CD4+ and CD8+ T cell subsets were less in Mas-TRECK Tg mice than in WT mice (See **Fig. S4A** in the Online Repository). In contrast, the numbers within each subset in the LN without sensitization were comparable between WT and Mas-TRECK Tg mice (See **Fig. S4A** in the Online Repository).

To evaluate of T cell differentiation after sensitization, the skin-draining LN cells from control or DNFB-sensitized WT and Mas-TRECK Tg mice were challenged in the presence or absence of DNBS *in vitro*. The incorporation of ^{3}H-thymidine and the levels of IFN-γ and IL-17 in the culture supernatant in the presence of DNBS were markedly decreased in LN cells from Mas-TRECK Tg mice as compared with those from WT mice (See **Fig. S4B-D** in the Online Repository). The levels of IL-4 in the culture supernatants were below the limit of detection of ELISA (<0.3 pg/mL).

Attenuated DC migration and maturation in the skin-draining LNs of Mas-TRECK Tg mice

An essential step in the sensitization phase for CHS is the migration of hapten-bearing cutaneous dendritic cells (DCs), such as epidermal Langerhans cells (LCs) and dermal DCs, into skin-draining lymph nodes (LNs). Accordingly, to dissect the site of

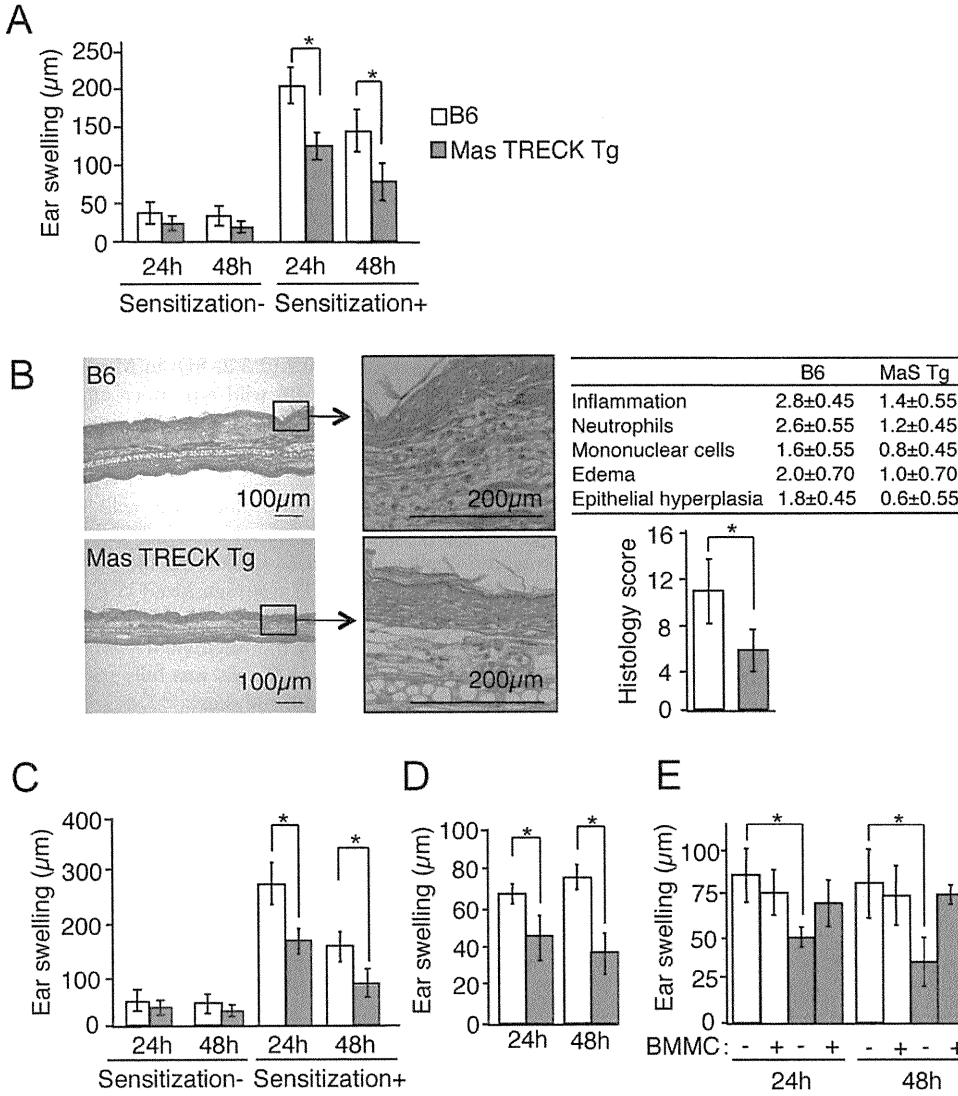

	B6	MaS Tg
Inflammation	2.8±0.45	1.4±0.55
Neutrophils	2.6±0.55	1.2±0.45
Mononuclear cells	1.6±0.55	0.8±0.45
Edema	2.0±0.70	1.0±0.70
Epithelial hyperplasia	1.8±0.45	0.6±0.55

Figure 1. MCs are essential during the sensitization phase in CHS. (A) Twelve days after DT treatment, WT and MaS TRECK Tg mice ($n = 12$ per group) were sensitized with or without DNFB and the ear swelling was measured 24 and 48 h after challenge with DNFB. (B) HE staining of the ears of sensitized DT-treated WT and MaS TRECK Tg mice 24 h after challenge with DNFB. Scale bar, 100 μm (left panels) and 200 μm (middle panels). Samples were scored for the severity and character of the inflammatory response using a subjective grading scale. The total histology score was calculated as the sum of scores (right panels). (C) Oxazolone-induced CHS in WT (white columns) and Mas-TRECK Tg (grey columns) mice. DT-treated WT and MaS TRECK Tg mice ($n = 13$ per group) were sensitized with oxazolone and ear swelling measured 24 and 48 hours after challenge with oxazolone. (D) CHS induced by adoptive transfer of LN cells sensitized with DNFB of WT (white columns) and Mas-TRECK Tg (grey columns) ($n = 6$ per group). (E) Draining LNs from oxazolone-sensitized WT (white columns) and Mas-TRECK Tg (grey columns) reconstituted with BMMCs ($n = 5$ per group) were adoptively transferred to induce CHS. All data are presented as the mean ± SD and are representative of three experiments. *, $P<0.05$ versus corresponding mice.
doi:10.1371/journal.pone.0025538.g001

action of MCs in the sensitization phase, we initially focused on cutaneous DCs that have an opportunity to interact with MCs present in the dermis.

Using a FITC-induced cutaneous DC migration model, we found that the numbers of both FITC$^+$ CD11c$^+$ MHC class II$^+$ CD207$^+$ DCs and FITC$^+$ CD11c$^+$ MHC class II$^+$ CD207$^-$ DCs in the draining LNs 24 h and 72 h after FITC application were significantly attenuated in Mas-TRECK Tg mice compared to WT mice (**Fig. 2A, B**). In addition, the numbers of total CD4$^+$ and CD8$^+$ T cells, and CD44$^+$ CD62L$^+$ central memory and CD44$^+$ CD62L$^-$ effector memory T cells in the draining LNs of Mas-TRECK Tg mice were less than those of WT mice (**Fig. 2C**). We next analyzed the expression levels of costimulatory molecules by skin organ culture. We incubated the skin and analyzed the expression levels on crawl-out DCs in the culture medium. The expression levels of CD40, CD80, and CD86 both on CD11c$^+$ MHC class II$^+$ EpCAM$^+$ LCs and CD11c$^+$ MHC class II$^+$ EpCAM$^-$ dermal DCs in Mas-TRECK Tg mice were lower than those of WT mice (**Fig. 2D, E,** and see **Fig. S5A**, upper panel, in the Online Repository). On the other hand, the expression levels of costimulatory molecules on LCs and dermal DCs from the untreated WT controls and Mas TRECK Tg mice were comparable (See **Fig. S5A**, lower panel, in the Online Repository). In addition, the expression levels on LCs and dermal DCs from WT and Mas-TRECK mice were comparable under steady state conditions (See **Fig. S5B** in the Online Repository).

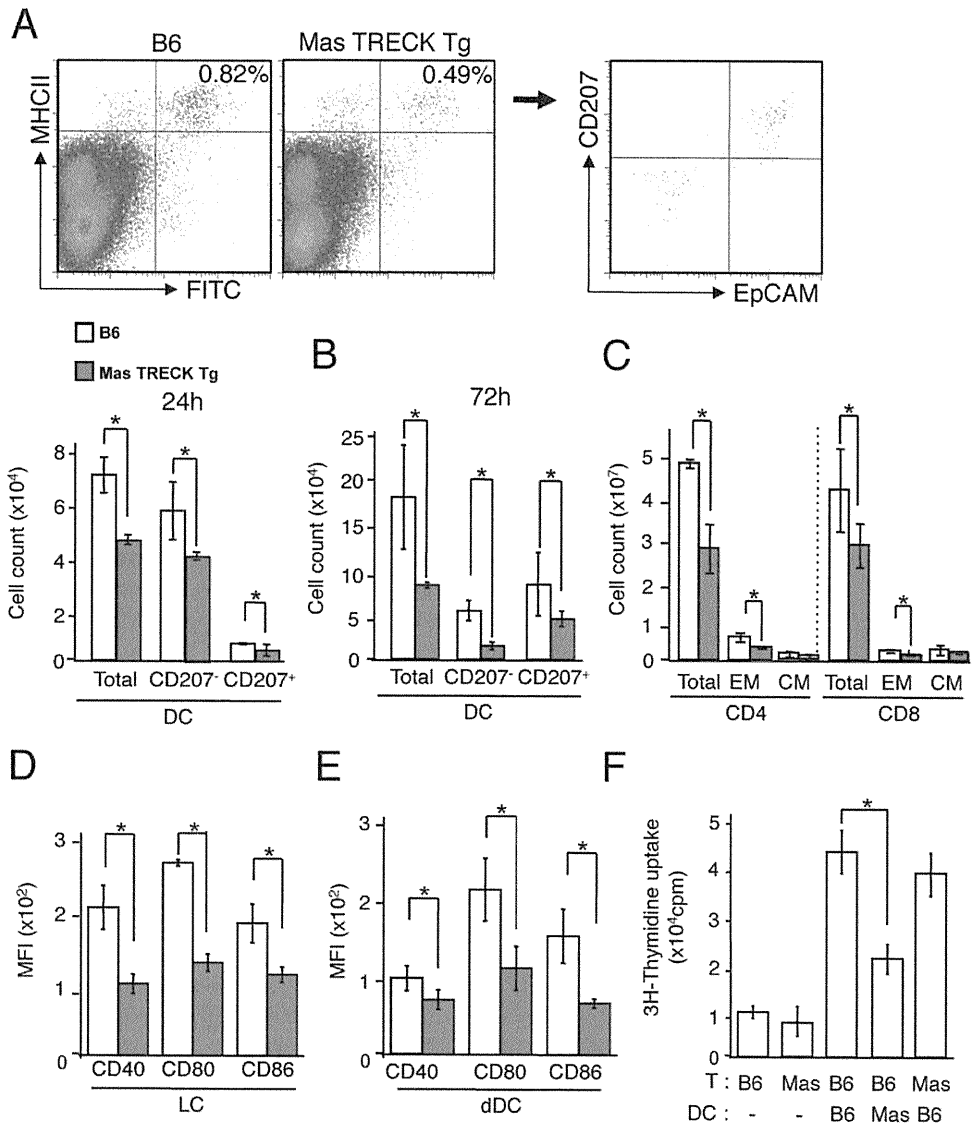

Figure 2. Impaired cutaneous DC migration and maturation in Mas-TRECK Tg mice. (A, B) The numbers of FITC$^+$ CD11c$^+$ MHC class II$^+$ CD207$^+$ DCs and FITC$^+$ CD11c$^+$ MHC class II$^+$ CD207$^-$ DCs in the draining LNs of DT-treated MaS TRECK Tg and WT mice 24 h and 72 h after application of FITC. (**C**) The numbers of total, central memory (CM), and effector memory (EM) CD4$^+$ and CD8$^+$ T cells in the draining LN 72 h after FITC application are shown. (D, E) The expression levels of CD40, CD80, and CD86 on both LCs and dDCs of DT-treated MaS TRECK Tg and WT mice. (F) *In vitro* assay of T-cell proliferation induced by DCs sorted from the draining LN of sensitized mice of WT or Mas-TRECK Tg (Mas) mice. Oxazolone-sensitized CD90.2$^+$ T cells were purified from the draining LNs of WT or Mas-TRECK Tg (Mas) mice 5 d after oxazolone application. T cells (5×10^5 cells) were incubated for 72 h, pulsed with 0.5 μCi [^{3}H]thymidine for the last 24 h ,with or without CD11c$^+$ DCs (1×10^5 cells) prepared from the draining LNs of DT-treated WT and MaS TRECK Tg mice one day after oxazolone application. All data are presented as the mean ± SD and are representative of three experiments. *, $P<0.05$ versus a corresponding group.
doi:10.1371/journal.pone.0025538.g002

Consistently, LCs and dermal DCs from *Kit*+/+ mice were similar to those from *Kit* $^{W/Wv}$ mice (See **Fig. S5B** in the Online Repository).

We further evaluated the effect of MCs on the antigen presenting capacity of DCs. We sorted 5×10^5 T cells by auto MACS from the draining LNs of CD90.2$^+$ WT mice five days after 25 μl of 2% oxazolone application. These CD90.2$^+$ T cells were incubated for 72 h with or without CD11c$^+$ DCs (1×10^5 cells) prepared from the draining LNs of WT or Mas-TRECK Tg mice one day after oxazolone application. T cell proliferation was enhanced by the addition of antigen-acquired DCs sorted from the draining LN of sensitized mice, and the extent of augmentation by DCs from WT mice was much higher than that of DCs from Mas-TRECK Tg mice (**Fig. 2F**).

Enhancement of BMDC maturation and chemotaxis by BMMC requires cell-cell contact in vitro

Impairment of DC functions as a result of MC deficiency suggests that MCs stimulate cutaneous DCs. To address this hypothesis, we prepared BMDCs [20] and incubated them with or without BMMCs. Co-cultivation of BMDCs with BMMCs for 24 h significantly increased the expression levels of CD40, CD80, CD86 and CCR7 on BMDCs (**Fig. 3A**). In addition the chemotaxis of BMDCs to CCL21 was significantly enhanced,

when BMMCs were added to the upper chamber with BMDCs (**Fig. 3B**).

Furthermore addition of BMMCs to the upper chamber of transwells did not induce further up-regulation of CD40, CD80, CD86 and CCR7 levels on BMDCs incubated in the lower chamber (**Fig. 3C**), which suggests that BMMCs require direct cell-cell interaction to stimulate BMDCs.

Stimulation of BMMCs by activated BMDCs

We then examined *in vitro* whether DCs directly contacted MCs. We incubated BMMCs and BMDCs, and found that c-kit$^+$ BMMCs contacted MHC class II$^+$ BMDCs (**Fig. 4A**). A number of FcεRIα$^+$ CD11c$^-$ MCs co-localized with CD11c$^+$ DCs in ear dermis 24 h after sensitization with DNFB (**Fig. 4B**). Consistent with this, the number of MCs co-located with DCs after sensitization was higher than that in the steady state (in other words, in non-inflammatory conditions) (4±0.81 vs 0.3±0.58; average ± SD).

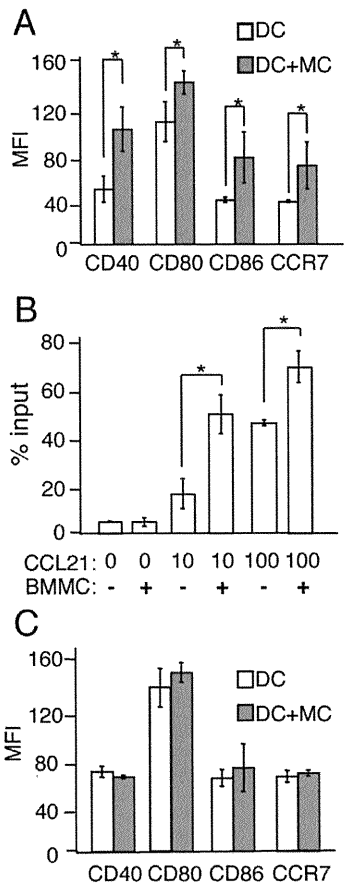

Figure 3. BMMCs promote the maturation and chemotactic activity of BMDCs via direct cell interaction. (A) The expression levels of CD40, CD80, CD86 and CCR7 on BMDCs cultured with or without BMMCs for 24 h. (B) Mobility of BMMCs to CCL21. BMMCs with or without BMDCs were applied to the upper chamber of a transwell without coating for 3 h. The numbers of MHC class II$^+$ cells in the lower chamber, identified as migrating DCs, were counted by means of flow cytometry. (C) The expression levels of CD40, CD80, CD86 and CCR7 on BMDCs cultured with or without BMMCs separately by using transwell culture plates for 24 h. All data are presented as the mean ± SD and are representative of three experiments. *, $P<0.05$ versus a corresponding group.
doi:10.1371/journal.pone.0025538.g003

At present, several stimuli in addition to IgE are known to trigger calcium influx and activate MCs [21]. Therefore, we studied the effect of BMDCs on BMMCs using Ca^{2+} imaging. We incubated tetramethylrhodamine ethyl ester (TMRE)-labeled BMDCs and Fluo-8-labeled BMMCs together. When an intracellular Ca^{2+} concentration of Fluo-8 (green) -labeled BMMCs is upregulated, fluorescence intensity of green becomes increased. Unstimulated CD11c$^+$ MHC class II^{int+} BMDCs did not increase BMMC intracellular Ca^{2+} concentrations (**Fig. 4C,** See **Video S1** in the Online Repository). On the other hand, stimulated CD11c$^+$ MHC class II^{high+} BMDCs induced prominent Ca^{2+} increase in BMMCs (**Fig. 4D** and See **Video S2** in the Online Repository). This rapid rise occurred five to ten times in 1000 seconds, and each spike lasted about 10–20 sec (**Fig. 4E**). Stimulated BMDCs significantly upregulated the ratio of BMMCs with increased Ca^{2+} concentration compared to non-stimulated BMDCs (**Fig. 4F**). These results suggest that stimulated DCs activate MCs via direct cell-cell contact.

Stimulation of DCs by MCs is dependent on ICAM-1-LFA-1 interaction and on MC membrane-bound TNF-α

We then sought to identify how MCs promote DC maturation. It has been reported that ICAM-1 on the surface of MCs directly interacts with leukocyte function-associated antigen 1 (LFA-1) on T cells, and that stimuli such as CD40L, LPS, and TNF-α, upregulate the expression of ICAM-1 on DCs [22]. In fact, the expression of ICAM-1 on BMDCs was up-regulated upon stimulation of BMDCs by LPS and CCL21 (**Fig. 5A**). Therefore, we hypothesized that MCs and DCs interact in an ICAM-1- and LFA-1-dependent manner. Addition of neutralizing anti-ICAM-1 antibody to a culture of BMDCs completely inhibited upregulation of CD40, CD80 and CD86 expression on BMDCs upon addition of BMMC (**Fig. 5B, S6A**).

We then analyzed intracellular signaling using the protein kinase A inhibitor, H89, and the phosphoinositide 3 kinase inhibitor, wortmannin. Although H89 did not inhibit the BMMC-induced upregulation of co-stimulatory molecules on BMDCs, wortmannin inhibited DC maturation (**Fig. 5C, S6B**). These results suggest that binding of ICAM-1 to LFA-1 activates DCs through a PI3-kinase pathway.

Lastly we tried to identify how DCs induce MC activation. TNF-α is first produced as a 26 kDa transmembrane molecule (membrane-bound TNF-α), which is cleaved by the metalloproteinase-disintegrin TNF-α converting enzyme TACE [23] to generate a soluble 17 kDa TNF-α. Studies have shown that membrane-bound TNF-α is also biologically active [24]. We first observed that anti-TNF-α antibody completely blocked DC maturation induced by BMMCs (**Fig. 5B**). Consistently, BMMC from TNF-α KO mice did not promote BMDC maturation (**Fig. S6C**). But the soluble form of TNF-α in the supernatant of co-cultures of BMMCs and TNF-α KO-derived BMDCs was below the detection limit irrespective of BMDC stimulation (<8 pg/ml, each). On the other hand, the level of membrane-bound TNF-α on BMMCs was increased by the addition of BMDCs and even further enhanced when stimulated BMDCs were added (**Fig. 5D**). These results suggest that MCs express membrane-bound TNF-α upon direct interaction with activated DCs through ICAM-1 on DCs and that membrane-bound TNF-α induces expression of co-stimulatory molecules on DCs.

Discussion

In this study, we used Mas-TRECK Tg mice in which MCs can be eliminated specifically and conditionally, and demonstrated

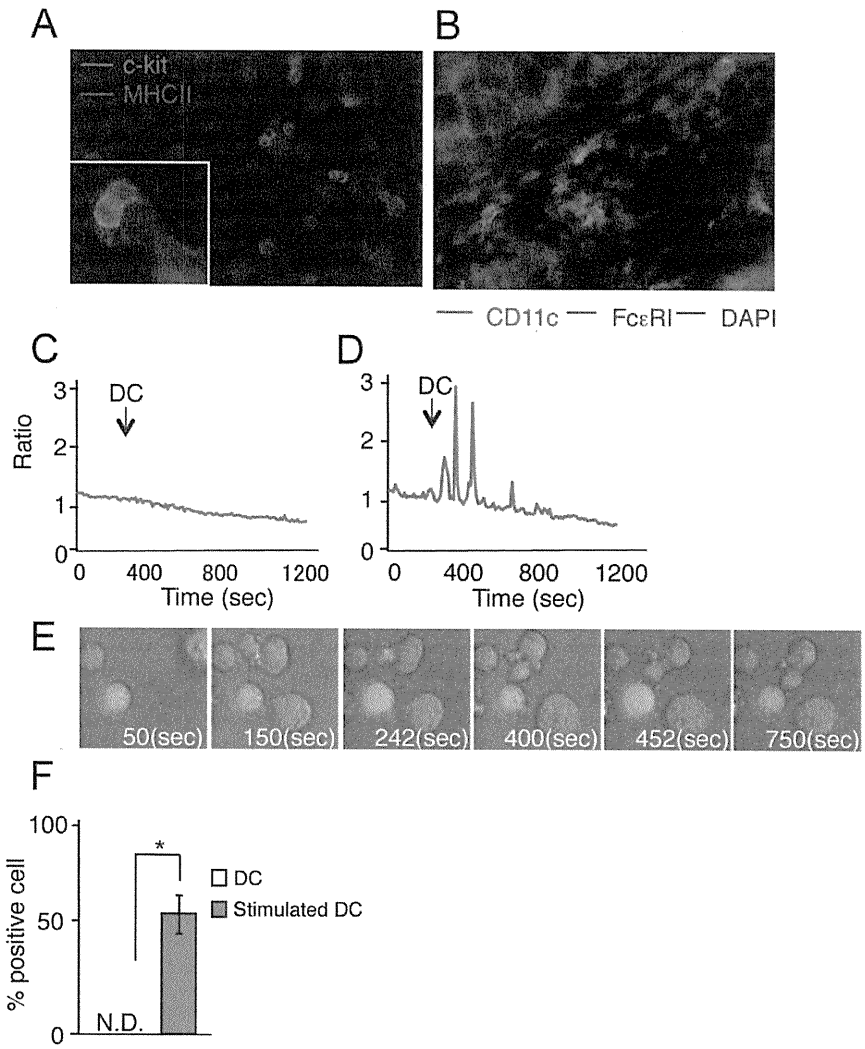

Figure 4. Stimulated BMDCs enhance Ca^{2+} influx in BMMCs and BMMCs interact with DCs in vitro and in vivo. (A) On poly-L-lysine coated glass coverslips, c-kit^{+} BMMCs (green) contacted MHC class II^{+} BMDCs (red). (B) Conjugate formation of CD11c^{+} DCs (green) with FcεRIα^{+} MCs (red) in the sensitized skin. (C–E) BMMCs (green) were co-cultured with non-stimulated BMDCs (C) or BMDCs stimulated with 100 ng/ml of LPS and 50 ng/ml of CCL21 for 1 h (red; D, E), and the intracellular Ca^{2+} was monitored by Fluo-8 for 1200 sec. Photos were taken at the indicated time points from Supplemental Movie 2 (E). (F) The percentage of BMMCs demonstrating high Ca^{2+} concentration among BMMCs. Data are presented as the mean ± SD and are representative of three experiments. *, $P<0.05$ versus a corresponding group.
doi:10.1371/journal.pone.0025538.g004

that CHS was significantly attenuated in accord with impaired memory T cell induction in skin-draining LNs after sensitization. MC depletion also impaired hapten-induced cutaneous DC migration concordant with levels of co-stimulatory molecule expression. In addition, BMMCs promoted BMDC maturation and chemotactic activity by direct interaction via ICAM-1 and membrane-bound TNF-α. In fact, a certain number of DCs were found colocalized with MCs in the DNFB-sensitized dermis. These findings suggest that MCs may promote migration and maturation of dermal DCs and epidermal LCs to establish the sensitization phase of CHS.

It was previously reported that FITC-induced cutaneous DC migration was attenuated in $Kit^{W\text{-}sh/KitW\text{-}sh}$ mice at 24 h, but not at 48 or 72 h after FITC application, and that the sensitization phase of CHS was not attenuated in $Kit^{W\text{-}sh/KitW\text{-}sh}$ mice [11]. The above findings were inconsistent with our findings in the way that cutaneous DC migration was attenuated even at 72 h after FITC application and that sensitization phase was impaired in Mas-TRECK Tg mice. On the other hand, it has also been shown that MCs are capable of influence both the sensitization phase and the elicitation phase in other models of CHS [25]. Therefore, it still remains unknown how the discrepancy occurred. The difference between our model and $Kit^{W/Wv}$ and $Kit^{W\text{-}sh/KitW\text{-}sh}$ mice is the existence of melanocytes and hematopoietic stem cells. Recently, melanocytes were shown to express toll like receptors, to modulate immune responses and to produce IL-1a and IL-1b [16,17]. In addition, because of congenital absence of MCs in $Kit^{W/Wv}$ and $Kit^{W\text{-}sh/KitW\text{-}sh}$ mice, compensatory mechanism may exist, such as repopulation of basophils. In fact, the numbers of basophils have been counted in these mice; the number of basophils in in $Kit^{W/Wv}$ mice are lower than that in WT mice, and that in $Kit^{W\text{-}sh/KitW\text{-}sh}$ mice are higher than that in WT mice [26]. These results indicate that the compensatory mechanisms may affect the result of CHS responses and that $Kit^{W/Wv}$ and $Kit^{W\text{-}sh/KitW\text{-}sh}$ mice may not necessarily be representative to evaluate the roles of pure MCs. In this study, we have demonstrated that the attenuated CHS response in Mas TRECK Tg mice was fully restored by the pre-engraftment of BMMCs into the skin just before sensitization with

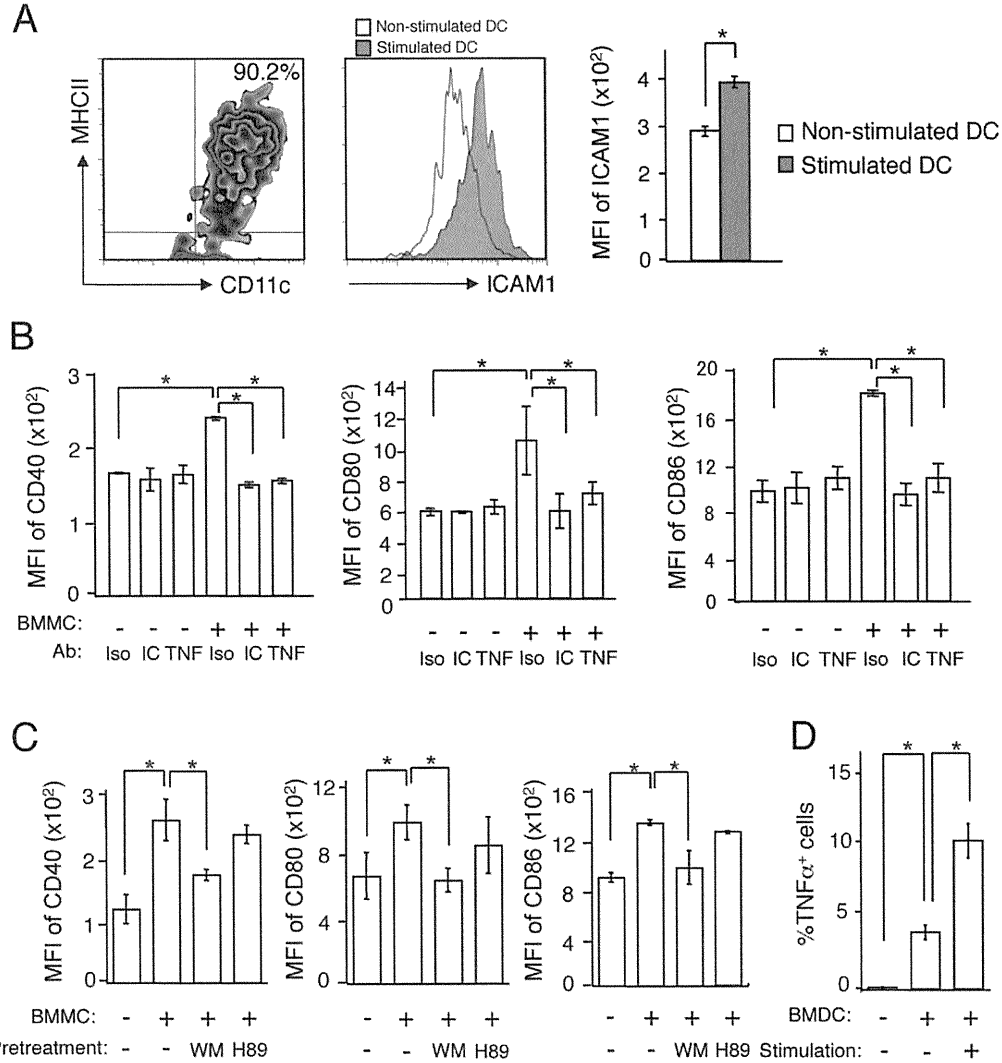

Figure 5. DC stimulation depends on ICAM-1-LFA-1 signals and membrane-bound TNF-α on MCs. (A) The expression of ICAM-1 on stimulated or non-stimulated BMDCs. (B, C) The expression levels of CD40, CD80, and CD86 on BMDCs co-cultured with BMMCs with isotype control Ab (Iso), anti-ICAM-1 Ab (IC), or anti-TNF-α Ab (TNF) (B), or co-cultured with BMMCs that were pretreated with or without wortmannin (WM) or H89 (C). (D) BMMCs expressing membrane-bound TNF-α in the presence of absence of BMDCs with or without stimulation with 100 ng/ml of LPS and 50 ng/ml of CCL21 for 1 h. All data are presented as the mean ± SD and are representative of three experiments. *, $P<0.05$.
doi:10.1371/journal.pone.0025538.g005

hapten. It is intriguing to evaluate this recovery by means of reconstitution with native skin MCs, since freshly generated BMMC and native skin MCs can differ in aspects of phenotype and function. We can't perform long term engraftment of BMMC in this model because we have found that repeated DT treatment (more than 5 days of daily injection) leads to weak viability of the Mas TRECK Tg mice.

We showed that co-culture of DCs with MCs did not promote soluble TNF-α secretion from MCs but up-regulated membrane-bound TNF-α on MCs. Since TNF-α expressed on MCs in this context is membrane-bound, MCs are required to co-localize with DCs *in vivo* to elicit its effect. Since neutralizing anti-TNF-α Ab abrogated the BMMC-induced DC maturation, membrane-bound TNF-α on MCs might be the major modulator of DC maturation. Herein we have focused on the roles of MCs in the sensitization phase, but we also noted that MC depletion in the elicitation phase attenuated the CHS response. Since DCs are thought to present antigen to memory T cells to initiate the challenge phase of CHS, the interaction of MCs and DCs might be essential for its establishment, which is a question that will be pursued in a future study.

The direct interaction between DCs and MCs was essential not only for DC stimulation, but also for MC activation. Previous reports have demonstrated that MCs contact extracellular matrix components to provide a co-stimulatory signal for histamine and cytokine production via integrins [27]. MCs are known to degranulate upon binding of ICAM-1 on MCs and LFA-1 on activated T cells [28]. In agreement with this, our study demonstrates that the interaction of MCs with DCs is dependent on cell-cell contact via ICAM-1 and LFA-1. In addition, an influx of calcium in MCs is induced by activated DCs that express high levels of ICAM-1, but not by immature DCs. Therefore, in sensitized skin, activated DCs bind to MCs and promote activation and up-regulating membrane-bound TNF-α on MCs. Activated MCs further promote additional activation of hapten-bearing cutaneous DCs causing them to migrate into skin-draining LNs. These findings indicate that MCs play an essential role in

establishing the sensitization phase of CHS by promoting cutaneous DC functions.

Materials and Methods

Mice

Mice expressing the human DTR under the control of IE element (for Mas-TRECK) and 3′UTR element (for Bas-TRECK) in the *Il4* locus were generated by a transgenic strategy. The basic pIL-4 construct was made by insertion of the 5′enhancer (5′E) (−863 to −5448; start codon is defined as sequence number 0) [29] and the IL-4 promoter from position −64 to −827. Human DTR fragment was isolated from human DTR/pMS7 vector that was provided by Dr. M. Tanaka (RCAI, RIKEN, Yokohama, Japan) and inserted into the basic pIL-4 construct. IE (+311 to +3534) and 3′UTR (+6231 to +10678) fragments were isolated from a mouse YAC clone (catalog no. 95022; Research Genetics, Huntsville, AL) and inserted into the basic pIL-4 and human DTR construct respectively. Each transgenic (Tg) line was generated on a C57BL/6 background. C57BL/6 (B6, WT) mice were purchased from Japan SLC (Shizuoka, Japan). TNF-α KO mice on the C57BL/6 background were generated [30]. WBB6F1-*Kit*+/+ and -*Kit* $^{W/W^v}$ mice were obtained from The Jackson Laboratory. For DT treatment, mice were injected intraperitoneally with 250 ng of DT in 250 µl of PBS per mouse for five consecutive days. Eight to ten week-old female mice were used for all the experiments and bred in specific pathogen-free facilities at Kyoto University. All experimental procedures were approved by the institutional animal care and use committee of Kyoto University Graduate School of Medicine (MedKyo11100).

Reagents, antibodies and intracellular staining

We purchased dinitrofluorobenzene (DNFB) from Nacalai Tesque (Kyoto, Japan), 2,4- dinitrobenzene sulfonic acid (DNBS) from Alfa Aesar (Ward Hill, MA). FITC-, PE-, PE-Cy5-, PE-Cy7-, APC-, APC-7-, and Pacific Blue-conjugated 145-2C11 (anti-CD3), GK1.5 (anti-CD4), 53-6.7 (anti-CD8), N418 (anti-CD11c), 1C10 (anti-CD40), 30-F11 (anti-CD45), 16-10A1 (anti-CD80), GL1 (anti-CD86), M5/114.15.2 (anti-MHC class II), MEL-14 (anti-CD62L), IM7 (anti-CD44), eBioKAT-1 (anti-intercellular adhesion molecule 1 (ICAM-1)), eBioL31 (anti-CD207), RB6-8C5 (anti-Gr-1), 4B12 (anti-CCR7)(eBioscience, San Diego, CA), and G8.8 (anti-EpCAM) (BioLegend, San Diego, CA) were purchased.

For Langerin (CD207) staining, cells were fixed and permeabilized with cytofix/cytoperm solution (BD Biosciences, San Jose, CA), and stained with biotin-conjugated anti-Langerin Ab. Cells were analyzed with FACSCantoII (BD, Franklin Lakes, NJ).

Histology and immunohistochemistry

Hematoxylin-eosin and toluidine blue staining [31], and the histological scoring were evaluated as reported [19]. In brief, samples were scored for the severity and character of the inflammatory response using a subjective grading scale. Responses were graded as follows: 0, no response; 1, minimal response; 2, mild response; 3, moderate response; and 4, marked response. The slides were blinded, randomized, and reread to determine the histology score. All studies were read by the same pathologist using the same subjective grading scale. The total histology score was calculated as the sum of scores, including inflammation, neutrophils, mononuclear cells, edema, and epithelial hyperplasia.

For immunohistochemistry, cryosections were fixed in acetone, incubated with hamster anti-mouse CD11c (eBioscience) followed by goat anti-hamster AlexaFluor488 (Invitrogen, Carlsbad, CA), and were subsequently incubated with PE-conjugated anti-mouse FcεRIα (eBioscience). Fluorescence images with DAPI staining were obtained using a BIOREVO BZ-9000 system (Keyence, Osaka, Japan).

Quantitative PCR analysis

Total RNAs were isolated with Trizol (Invitrogen) from ear skin. cDNA was reverse transcribed using a PrimeScript RT reagent kit (Takara Bio, Otsu, Japan). Quantitative RT-PCR with a Light Cycler real time PCR apparatus was performed (Roche Diagnostics, Foster City, CA) using SYBR Green I (Takara Bio). Primers for *Ifng*, *Il17*, and *Il1b* were obtained from Hokkaido System Science (Sapporo, Japan) and the primer sequences were *Ifng*, 5′- ATG AAC GCT ACA CAC TGC ATC -3′ (Forward) and 5′- CCA TCC TTT TGC CAG TTC CTC -3′ (reverse); *Il17*, 5′- TTT AAC TCC CTT GGC GCA AAA -3′ (forward), 5′- CTT TCC CTC CGC ATT GAC AC -3′ (reverse); and *Il1b*, 5′- GCA ACT GTT CCT GAA CTC AAC T -3′ (forward), 5′- ATC TTT TGG GGT CCG TCA ACT -3′ (reverse). For each sample, triplicate test reactions and a control reaction lacking reverse transcriptase were analyzed for expression of the genes and results were normalized to those of the 'housekeeping' glyceraldehyde-3-phosphate dehydrogenase (*Gapdh*) levels.

Lymphocyte proliferation assay and cytokine production

For DNBS-dependent proliferation, single-cell suspensions from skin-draining LNs of mice 5 days after sensitization with DNFB. One million LN cells were cultured with or without 100 µg/ml of DNBS for 72 h, pulsed with 0.5 µCi 3H-thymidine for the last 24 h, and subjected to liquid scintillation counting.

For measurement of cytokine production, the culture supernatants were collected 72 h after incubation and were measured by ELISA (BD Biosciences and R&D systems, Minneapolis, MN) according to the manufacture's protocol.

CHS protocol

Mice were sensitized with 50 µl of 0.5% (w/v) DNFB in acetone/olive oil (4/1) or 2% oxazolone (Wako Pure Chemical Industries, Ltd, Osaka, Japan) in ethanol on abdominal skin. On day 5, the ears were challenged by application of 20 µl of 0.3% DNFB or 1% oxazolone.

For adoptive transfer, LN cells were prepared from the inguinal and axillary LNs of one mouse sensitized with DNFB 5 days previously, and transferred intravenously into a mouse. The ears of these animals were challenged with 20 µl of 0.3% DNFB 1 h later, and the ear thickness change was measured. For adoptive transfer of T cells, T cells purified with CD90.2$^+$ microbeads (Miltenyi Biotec, Bergisch Gladbach, Germany) were prepared from the inguinal and axillary LNs of a mouse sensitized with 2% oxazolone 5 days previously, and transferred intravenously into a mouse. The ears of these animals were challenged with 20 µl of 1% oxazolone 1 h later, and the ear thickness change was measured.

Generation of BMDC and BMMC

Complete RPMI (cRPMI), RPMI 1640 medium (Sigma, St. Louis, MO) containing 10% fetal calf serum (Invitrogen), was used as culture medium. For BMDC induction, 5×10^6 BM cells were cultured supplemented with 10 ng/ml recombinant murine GM-CSF (PeproTech, Rocky Hill, NJ) for five days [20] (>90% expressed CD11c).

For BMMC induction, 1×10^6 BM cells were cultured supplemented with 5 ng/ml recombinant murine SCF and IL-3 (PeproTech) for more than three weeks (>98% expressed c-kit and FcεRIα).

For organ culture assay, the skin from mouse ears was split along with cartilage, and the dorsal ear skin without cartilage was floated in a dermal side-down manner in 24-well tissue culture plates. Twenty-four hours later, the cells in the wells were collected for analysis.

Chemotaxis assay and FITC-induced cutaneous DC migration

Cells were tested for transmigration to CCL21 (R&D Systems) or medium in the lower chamber across uncoated 5-μm transwell filters (Corning Costar Corp., Corning, NY) for 6 h and were enumerated by flow cytometry.

For FITC-induced cutaneous DC migration, mice were painted on the shaved abdomen with 100 μl of 2% FITC (Sigma) dissolved in a 1:1 (v/v) acetone/dibutyl phthalate (Sigma) mixture, and the number of migrated cutaneous DCs into draining LNs was enumerated by flow cytometry.

Co-culture of BMDCs and BMMCs

BMDCs and starved BMMCs were co-cultured at a density of 2×10^5 DCs in 200 μl per well in a 96-well microplate at a DC:MC ratio of 2:1 and the co-culture was performed for 24 h. Separation of BMDCs and BMMCs was performed by using transwell culture plates with a 3-μm pore size (Costar, Corning). To observe cell-cell contact *in vitro*, BMDCs and BMMCs were co-cultured on poly-L-lysine coated glass coverslips (ASAHI GLASS Co., LTD, Tokyo, Japan) for 24 h and stained with FITC-conjugated anti-c-Kit and PE-conjugated anti-MHC class II.

For inhibition assays, BMDCs and starved BMMCs were co-cultured with or without 5 μg/ml of isotype control Ab (Rat IgG2b, eBioscience), 20 μg/ml of anti-ICAM-1 Ab (YN1/1.7.4, eBioscience) or 5 μg/ml of anti-TNF-α Ab (MP6-XT22, eBioscience) for 24 h. Starved BMMCs were pretreated with or without wortmannin (100 nM; Sigma) or H89 (10 mM; Sigma) for 1 h and then co-cultured with BMDCs for 24 h.

For detection of membrane-bound TNF-α, starved BMMCs were cultured for 24 h with or without non-stimulated or stimulated BMDCs with 100 ng/ml of LPS (Sigma) and 50 ng/ml of CCL21 (R&D systems) for 1 h.

Cytoplasmic Ca^{2+} imaging

BMMCs were incubated with 5 mM Quest Fluo-8 AM (ABD Bioquest, CA, USA), and BMDCs were stimulated with 100 ng/ml of LPS and 50 ng/ml of CCL21 for 1 h and stained with 2.5 nM tetramethylrhodamine ethyl ester (TMRE) (Invitrogen). The Fluo-8 image and the transmission image were recorded every 10 sec using a back-thinned electron multiplier CCD camera (ImagEM, Hamamatsu Photonics, Japan) and microscope (Eclipse Ti, Nikon, Japan). The fluorescence intensity was expressed as a ratio to the initial value after subtracting background fluorescence.

Statistical analysis

Unless otherwise indicated, data are presented as the means ± standard deviation (SD) and are a representative of three independent experiments. *P*-values were calculated with the two-tailed Student's *t*-test or one-way ANOVA followed by the Dunnett multiple comparison test. *P* values less than 0.05 are considered to be significantly different between MasTRECK and corresponding WT mice and are shown as * in the figures.

Supporting Information

Figure S1 Effect of DT on MC in Mas-TRECK Tg mice. (A) Skin MCs in Mas-TRECK Tg mice were stained with toluidine blue with (left panel) or without (right panel) DT treatment. The numbers of skin MCs in Mas-TRECK Tg mice with or without DT treatment under steady state or inflammatory conditions (after 24 hours CHS response) are shown (lower). n.d., not detected (n = 5). (B) WT and Mas-TRECK Tg mice ($n = 5$) were treated with DT, and DCs ($CD11c^+$), B cells ($B220^+$), NK cells ($DX5^+$ $Fc\varepsilon RI^-$), NKT cells ($CD3^+DX5^+$), $CD4^+$ T cells ($CD3^+CD4^+$), $CD8^+$ T cells ($CD3^+CD8^+$), eosinophils and neutrophils ($Gr\text{-}1^+$) were obtained from PBMCs 12 days later (left). WT and Mas-TRECK Tg mice ($n = 5$) were treated with DT, and the numbers of basophils ($DX5^+Fc\varepsilon RI^+$) per ml in PBMCs were evaluated 5 days and 12 days later (right). All data are presented as the mean ± SD and are representative of three experiments.
(PDF)

Figure S2 CHS responses in *Kit* $^{W/W^v}$ and Bas-TRECK mice. (A) DNFB-induced CHS in WBB6F1-*Kit*+/+ and WBB6F1-*Kit* *Kit* $^{W/W^v}$ mice. WBB6F1-*Kit*+/+ and WBB6F1-*Kit* *Kit* $^{W/W^v}$ mice were sensitized with or without DNFB and the ear swelling was measured 24 and 48 h after challenge with DNFB ($n = 10$ per group). (B) DNFB-induced CHS in DT-treated WT and Bas-TRECK Tg mice. DT-treated WT and Bas-TRECK Tg mice were sensitized with or without DNFB and the ear swelling was measured 24 and 48 h after challenge with DNFB ($n = 10$ per group). (C) Oxazolone-induced CHS in DT-treated WT and Mas-TRECK Tg mice. Mice were sensitized with 5% oxazolone and challenged with 1% oxazolone at the high hapten dose ($n = 10$ per group). (D) CHS induced by adoptive transfer of $CD90.2^+$ T cells from WT and Mas-TRECK Tg mice sensitized with DNFB ($n = 6$ per group). (E) Toluidine blue positive mast cells in the skin with Mas TRECK Tg mice or B6 wild type mice after one hour injection of BMMC (n = 3). All data are presented as the mean ± SD and are representative of three experiments. *, $P<0.05$ versus a corresponding group.
(PDF)

Figure S3 Decreased infiltrating cells and cytokines in the skin of Mas-TRECK Tg mice after challenge. (A) The numbers of $CD4^+$ T cells, $CD8^+$ T cells and neutrophils ($CD45^+Gr\text{-}1^{high}$) in DNFB-challenged skin were counted in DT-treated Mas-TRECK Tg or WT mice ($n = 5$ per group) using flow cytometry. (B) mRNA levels of IFN-γ, IL-17 and IL-1β in the skin after CHS ($n = 5$ per group). All data are presented as the mean ± SD and are representative of three experiments.
(PDF)

Figure S4 Impaired development of the Th1 subset in CHS and decreased cytokine production in the LN of sensitized Mas-TRECK Tg mice. (A) Skin-draining LN cells were collected from MaS TRECK Tg and WT mice 5 days after DNFB application. The numbers of $CD44^{high}CD62L^+$central memory (CM) or $CD44^{high}CD62L^-$ effector memory (EM) cells and total $CD4^+$ and $CD8^+$ T cells in the draining LNs with or without sensitization are shown. (B-D) DNBS-induced lymphocyte proliferation (B) and cytokine production (C, D). Cells were collected from MaS TRECK Tg and WT mice 5 days after DNFB application and cultured for 3 days with or without 100 μg/mL DNBS. Cell proliferation was measured by ^{3}H-thymidine incorporation. The amounts of IFN-γ and IL-17 in the culture medium were measured by ELISA. $n = 10$ mice per group.
(PDF)

Figure S5 Attenuated DC maturation in the absence of MCs. (A) Representative flow cytometry profiles of the skin from WT and Mas TRECK Tg mice (left), and histogram of CD40 expression on LCs and dDCs from DT-treated WT mice and Mas-TRECK Tg mice treated with or without DT. (B) The

expression levels of CD40, CD80, and CD86 on LCs and dDCs in the ear skin from WBB6F1-*Kit*+/+, -*Kit* $^{W/W^v}$,WT, and Mas-TRECK Tg mice under steady state conditions.
(PDF)

Figure S6 timulation of DCs by MCs is dependent on ICAM-1-LFA-1 interaction and on MC membrane-bound TNF-α. (A, B) Histogram. The expression levels of CD40 on BMDCs co-cultured with BMMCs with isotype control Ab, anti-ICAM-1 Ab, or anti-TNF-α Ab (TNF) (A), or co-cultured with BMMCs that were pretreated with or without wortmannin (WM) or H89 (B). (C) The expression levels of CD40, CD80, and CD86 on BMDCs co-cultured with WT derived BMMCs or TNF-α KO (TNF KO) derived BMMCs.
(PDF)

Video S1 Quest Fluo-8 AM-stained BMMCs and TMRE-stained BMMCs were mixed on glass coverslips and recorded every 10 sec at ~30°C using a back-thinned electron multiplier CCD camera.
(MOV)

Video S2 Quest Fluo-8 AM-stained BMMCs and TMRE-stained stimulated BMMCs were mixed on glass coverslips and recorded every 10 sec at ~30°C using a back-thinned electron multiplier CCD camera.
(MOV)

Acknowledgments

We thank Dr. Heinrich Körner (Cellular Immunology Laboratory, Comparative Genomics Centre, James Cook University, Townsville, 4811, Queensland, Australia) and Dr. Hajime Suto (Atopy Research Center, Juntendo University School of Medicine, Tokyo, 113-8412, Japan) for kindly providing TNF-α KO mice.

Author Contributions

Conceived and designed the experiments: AO MK. Performed the experiments: AO BK SM. Analyzed the data: TH GE SN HT TW SN. Contributed reagents/materials/analysis tools: MK. Wrote the paper: YM KK.

References

1. Grabbe S, Schwarz T (1998) Immunoregulatory mechanisms involved in elicitation of allergic contact hypersensitivity. Immunol Today 19: 37–44.
2. Tomura M, Honda T, Tanizaki H, Otsuka A, Egawa G, et al. (2010) Activated regulatory T cells are the major T cell type emigrating from the skin during a cutaneous immune response in mice. J Clin Invest 120: 883–893.
3. Egawa G, Honda T, Tanizaki H, Doi H, Miyachi Y, et al. (2011) In Vivo Imaging of T-Cell Motility in the Elicitation Phase of Contact Hypersensitivity Using Two-Photon Microscopy. J Invest Dermatol.
4. Egawa G, Kabashima K (2011) Skin as a Peripheral Lymphoid Organ: Revisiting the Concept of Skin-Associated Lymphoid Tissues. J Invest Dermatol.
5. Kabashima K, Miyachi Y (2004) Prostanoids in the cutaneous immune response. J Dermatol Sci 34: 177–184.
6. Romani N, Clausen BE, Stoitzner P (2010) Langerhans cells and more: langerin-expressing dendritic cell subsets in the skin. Immunol Rev 234: 120–141.
7. Bursch LS, Wang L, Igyarto B, Kissenpfennig A, Malissen B, et al. (2007) Identification of a novel population of Langerin+ dendritic cells. J Exp Med 204: 3147–3156.
8. Honda T, Nakajima S, Egawa G, Ogasawara K, Malissen B, et al. (2010) Compensatory role of Langerhans cells and langerin-positive dermal dendritic cells in the sensitization phase of murine contact hypersensitivity. J Allergy Clin Immunol 125: 1154–1156 e1152.
9. Kitawaki T, Kadowaki N, Sugimoto N, Kambe N, Hori T, et al. (2006) IgE-activated mast cells in combination with pro-inflammatory factors induce Th2-promoting dendritic cells. Int Immunol 18: 1789–1799.
10. Jawdat DM, Albert EJ, Rowden G, Haidl ID, Marshall JS (2004) IgE-mediated mast cell activation induces Langerhans cell migration in vivo. J Immunol 173: 5275–5282.
11. Suto H, Nakae S, Kakurai M, Sedgwick JD, Tsai M, et al. (2006) Mast cell-associated TNF promotes dendritic cell migration. J Immunol 176: 4102–4112.
12. Kabashima K, Narumiya S (2003) The DP receptor, allergic inflammation and asthma. Prostaglandins Leukot Essent Fatty Acids 69: 187–194.
13. Hammad H, de Heer HJ, Soullie T, Hoogsteden HC, Trottein F, et al. (2003) Prostaglandin D2 inhibits airway dendritic cell migration and function in steady state conditions by selective activation of the D prostanoid receptor 1. J Immunol 171: 3936–3940.
14. Galli SJ, Hammel I (1984) Unequivocal delayed hypersensitivity in mast cell-deficient and beige mice. Science 226: 710–713.
15. Galli SJ, Grimbaldeston M, Tsai M (2008) Immunomodulatory mast cells: negative, as well as positive, regulators of immunity. Nat Rev Immunol 8: 478–486.
16. Yu N, Zhang S, Zuo F, Kang K, Guan M, et al. (2009) Cultured human melanocytes express functional toll-like receptors 2-4, 7 and 9. J Dermatol Sci 56: 113–120.
17. Swope VB, Sauder DN, McKenzie RC, Sramkoski RM, Krug KA, et al. (1994) Synthesis of interleukin-1 alpha and beta by normal human melanocytes. J Invest Dermatol 102: 749–753.
18. Yagi R, Tanaka S, Motomura Y, Kubo M (2007) Regulation of the Il4 gene is independently controlled by proximal and distal 3′ enhancers in mast cells and basophils. Mol Cell Biol 27: 8087–8097.
19. Nakajima S, Honda T, Sakata D, Egawa G, Tanizaki H, et al. (2010) Prostaglandin I2-IP signaling promotes Th1 differentiation in a mouse model of contact hypersensitivity. J Immunol 184: 5595–5603.
20. Tanizaki H, Egawa G, Inaba K, Honda T, Nakajima S, et al. (2010) Rho-mDia1 pathway is required for adhesion, migration, and T-cell stimulation in dendritic cells. Blood 116: 5875–5884.
21. Chang WC, Nelson C, Parekh AB (2006) Ca2+ influx through CRAC channels activates cytosolic phospholipase A2, leukotriene C4 secretion, and expression of c-fos through ERK-dependent and -independent pathways in mast cells. Faseb J 20: 2381–2383.
22. Cella M, Scheidegger D, Palmer-Lehmann K, Lane P, Lanzavecchia A, et al. (1996) Ligation of CD40 on dendritic cells triggers production of high levels of interleukin-12 and enhances T cell stimulatory capacity: T-T help via APC activation. J Exp Med 184: 747–752.
23. Black RA, Rauch CT, Kozlosky CJ, Peschon JJ, Slack JL, et al. (1997) A metalloproteinase disintegrin that releases tumour-necrosis factor-alpha from cells. Nature 385: 729–733.
24. Kriegler M, Perez C, DeFay K, Albert I, Lu SD (1988) A novel form of TNF/cachectin is a cell surface cytotoxic transmembrane protein: ramifications for the complex physiology of TNF. Cell 53: 45–53.
25. Bryce PJ, Miller ML, Miyajima I, Tsai M, Galli SJ, et al. (2004) Immune sensitization in the skin is enhanced by antigen-independent effects of IgE. Immunity 20: 381–392.
26. Piliponsky AM, Chen CC, Grimbaldeston MA, Burns-Guydish SM, Hardy J, et al. (2010) Mast cell-derived TNF can exacerbate mortality during severe bacterial infections in C57BL/6-KitW-sh/W-sh mice. Am J Pathol 176: 926–938.
27. Ra C, Yasuda M, Yagita H, Okumura K (1994) Fibronectin receptor integrins are involved in mast cell activation. J Allergy Clin Immunol 94: 625–628.
28. Inamura N, Mekori YA, Bhattacharyya SP, Bianchine PJ, Metcalfe DD (1998) Induction and enhancement of Fc(epsilon)RI-dependent mast cell degranulation following coculture with activated T cells: dependency on ICAM-1- and leukocyte function-associated antigen (LFA)-1-mediated heterotypic aggregation. J Immunol 160: 4026–4033.
29. Kubo M, Ransom J, Webb D, Hashimoto Y, Tada T, et al. (1997) T-cell subset-specific expression of the IL-4 gene is regulated by a silencer element and STAT6. EMBO J 16: 4007–4020.
30. Korner H, Cook M, Riminton DS, Lemckert FA, Hoek RM, et al. (1997) Distinct roles for lymphotoxin-alpha and tumor necrosis factor in organogenesis and spatial organization of lymphoid tissue. Eur J Immunol 27: 2600–2609.
31. Maurer M, Fischer E, Handjiski B, von Stebut E, Algermissen B, et al. (1997) Activated skin mast cells are involved in murine hair follicle regression (catagen). Lab Invest 77: 319–332.

PGD_2 induces eotaxin-3 via PPARγ from sebocytes: A possible pathogenesis of eosinophilic pustular folliculitis

Kyoko Nakahigashi, MD,[a] Hiromi Doi, MS,[a] Atsushi Otsuka, MD, PhD,[a] Tetsuya Hirabayashi, PhD,[b] Makoto Murakami, PhD,[b] Yoshihiro Urade, PhD,[c] Hideaki Tanizaki, MD, PhD,[a] Gyohei Egawa, MD, PhD,[a] Yoshiki Miyachi, MD, PhD,[a] and Kenji Kabashima, MD, PhD[a] *Kyoto, Tokyo, and Osaka, Japan*

Background: Eosinophilic pustular folliculitis (EPF) is a chronic intractable pruritic dermatosis characterized by massive eosinophil infiltrates involving the pilosebaceous units. Recently, EPF has been regarded as an important clinical marker of HIV infection, and its prevalence is increasing in number. The precise mechanism by which eosinophils infiltrate into the pilosebaceous units remains largely unknown. Given that indomethacin, a COX inhibitor, can be successfully used to treat patients with EPF, we can assume that COX metabolites such as prostaglandins (PGs) are involved in the etiology of EPF.
Objective: To determine the involvement of PGs in the pathogenesis of EPF.
Methods: We performed immunostaining for PG synthases in EPF skin lesions. We examined the effect of PGD_2 on induction of eotaxin, a chemoattractant for eosinophils, in human keratinocytes, fibroblasts, and sebocytes and sought to identify its responsible receptor.
Results: Hematopoietic PGD synthase was detected mainly in infiltrating inflammatory cells in EPF lesions, implying that PGD_2 was produced in the lesions. In addition, PGD_2 and its immediate metabolite 15-deoxy-Δ 12,14-PGJ_2 (15d-PGJ_2) induced sebocytes to produce eotaxin-3 via peroxisome proliferator–activated receptor gamma. Consistent with the above findings, eotaxin-3 expression was immunohistochemically intensified in sebaceous glands of the EPF lesions.
Conclusion: The PGD_2/PGJ_2-peroxisome proliferator–activated receptor gamma pathway induces eotaxin production from sebocytes, which may explain the massive eosinophil infiltrates observed around pilosebaceous units in EPF. (J Allergy Clin Immunol 2012;129:536-43.)

Key words: *Prostaglandin D_2, hematopoietic prostaglandin D synthase, eotaxin-3/CCL26, sebocyte, peroxisome proliferator–activated receptor gamma*

Abbreviations used
- CRT_H2: Chemoattractant receptor–homologous molecule expressed on T_H2 cells
- EPF: Eosinophilic pustular folliculitis
- GAPDH: Glyceraldehyde 3-phospate dehydrogenase
- H-PGDS: Hematopoietic prostaglandin D synthase
- L-PGDS: Lipocalin-type prostaglandin D synthase
- PG: Prostaglandin
- PPARγ: Peroxisome proliferator–activated receptor gamma
- siRNA: Small-interfering RNA

Eosinophilic pustular folliculitis (EPF) is a chronic intractable pruritic dermatosis characterized by massive eosinophil infiltrates involving the pilosebaceous units.[1] The evidence accumulated to date indicates that T_H2-mediated immunologic mechanisms are involved in the pathogenesis of EPF.[2,3] Recently, EPF has been regarded as an important clinical marker of HIV infection, and its prevalence is increasing in number.[4] An immunohistochemical study has demonstrated the expression of intercellular adhesion molecules for inflammatory cells including eosinophils around hair follicles.[5] Other studies have reported that IL-5 level, which induces proliferation and differentiation of eosinophils, is elevated in the blood and skin lesions of patients with EPF, but it can be decreased by treatment with IFN-γ.[6,7] Three members of the eotaxin family—eotaxin-1/CCL11, eotaxin-2/CCL24, and eotaxin-3/CCL26—are known to promote the growth and recruitment of eosinophils and skin inflammation.[8] T_H2 cytokines, such as IL-4, -5, and -13, enhance the production of eotaxins by skin component cells, such as lymphocytes, macrophages, endothelial cells, fibroblasts, and keratinocytes.[9-11] These findings suggest that the pathogenesis of EPF consists of a T_H2-type immune response; intriguingly, however, EPF is usually resistant to topical or systemic corticosteroids that suppress the functions of T cells. Therefore, the pathogenesis of EPF might not be explained solely by T_H2 immunity. Since EPF can be successfully treated with indomethacin, a COX inhibitor,[12] we hypothesize that the prostaglandin (PG) family known as the prostanoids, which occur downstream of COX, might be involved in the etiology of EPF.

Prostanoids are released from cells immediately after their formation. Because they are chemically and metabolically unstable, they usually function only locally through membrane receptors on target cells.[13] Recently, individual prostanoid receptor gene–deficient mice have been used as models to dissect the respective roles of each receptor in combination with the use of compounds that selectively bind to prostanoid receptors as agonists or antagonists.[14,15] The prostanoids PGD_2 and PGE_2 are 2 of the major COX metabolites in the skin. PGE_2 has been reported to have an inhibitory effect on eosinophil trafficking and

From [a]the Department of Dermatology, Graduate School of Medicine, Kyoto University, Kyoto; [b]the Lipid Metabolism Project, Tokyo Metropolitan Institute of Medical Science, Tokyo; and [c]the Department of Molecular Behavioural Biology, Osaka Bioscience Institute, Osaka.

This work was supported in part by Grants-in-Aid for Scientific Research from the Ministry of Education, Culture, Sports, Science and Technology, and Health and from the Ministry of Health, Labour and Welfare of Japan.

Disclosure of potential conflict of interest: The authors declare that they have no relevant conflicts of interest.

Received for publication August 5, 2011; revised October 21, 2011; accepted for publication November 23, 2011.

Available online December 28, 2011.

Corresponding author: Kenji Kabashima, MD, PhD, Department of Dermatology, Graduate School of Medicine, Kyoto University, 54 Shogoin-Kawara, Sakyo, Kyoto 606-8507, Japan. E-mail: kaba@kuhp.kyoto-u.ac.jp.

0091-6749/$36.00

doi:10.1016/j.jaci.2011.11.034

activation.[16] PGD_2, on the other hand, is known to be involved in chronic allergic inflammation.[17] Two types of PGD synthase (PGDS), which catalyzes the isomerization of PGH_2, a common precursor of various prostanoids that catalyze PGD_2, have been identified: one is the lipocalin-type PGDS (L-PGDS), and the other is the hematopoietic PGDS (H-PGDS).[18] L-PGDS is localized in the central nervous system, the male genital organs, the heart, and melanocytes in skin.[18,19] H-PGDS is widely distributed in the peripheral tissues and localized in antigen-presenting cells, mast cells, megakaryocytes, T_H2 lymphocytes, and dendritic cells.[18,20-22]

The aim of this study was to verify the hypothesis that prostanoids are involved in the development of eosinophil infiltration in the pilosebaceous units of the EPF skin lesions. We found that inflammatory cells in EPF lesions were positively immunostained for H-PGDS, suggesting that PGD_2 production was increased in EPF lesions. Moreover, we found that PGD_2 increased eotaxin-3 mRNA expression in sebocytes via peroxisome proliferator–activated receptor gamma (PPARγ) and that eotaxin-3 was detected around sebaceous glands in EPF lesions. Our data suggest that PGD_2 is involved in the pathogenesis of EPF lesions by inducing eotaxin-3 from sebocytes via PPARγ.

METHODS

Human subjects

We obtained biopsy specimens from 5 patients with EPF, 6 patients with folliculitis, and 4 healthy subjects. Informed consent was obtained from all subjects involved in this study. The Ethics Committee of Kyoto University approved the study.

Histologic examination

Paraffin-embedded sections were stained with hematoxilin-eosin and immunostained with H-PGDS, a monoclonal mouse antihuman antibody (dilution 1:500), L-PGDS, a polyclonal rabbit antihuman antibody (dilution 1:1000) (both were established at the Osaka Bioscience Institute, Osaka, Japan), and eotaxin-3/CCL26, a polyclonal goat antihuman antibody (dilution 1:100, R&D Systems, Minneapolis, Minn). As negative controls for H-PGDS and L-PGDS antibodies, we used isotype-matched control antibody and rabbit serum, respectively. Antigen retrieval was achieved by pepsin treatment for L-PGDS and preincubation with proteinase K for eotaxin-3. Nonspecific binding was blocked by addition of 10% goat serum for 30 minutes at room temperature. Afterward, sections were incubated for 1 hour at room temperature with the primary antibody followed by incubation with a species-specific biotinylated immunoglobulin (Vector, Burlingame, Calif) for 30 minutes at room temperature. Thereafter, they were incubated for 30 minutes with the avidine-biotin-peroxidase complex kit (Vector) and visualized with 3,3′-diaminobenzidine. They were lightly counterstained with hematoxylin. The number of immunoreactive cells per high power field was enumerated at 3 locations (original magnification ×200) per sample, and data were expressed as the number of H-PGDS– and L-PGDS–positive cells per high power field.

Preparation of human eosinophils and flow cytometry

Peripheral blood was obtained from 3 patients with EPF and 3 healthy donors. Polynuclear cells were separated by centrifugation of whole blood over Mono-Poly Resolving Medium (DS Pharma Biomedical, Osaka, Japan), followed by removal of remaining red cells by ACK lysing buffer (Lonza Walkersville, Inc, Walkersville, Md). They were stained with the antibodies against surface markers of eosinophils: antihuman CCR3-phycoerythrin (dilution 1:100, R&D Systems) and antihuman CD16-fluorescein isothiocyanate (dilution 1:100, Becton Drive Biosciences, Franklin Lakes, NJ). Eosinophils were identified with CCR3 positive and CD16 negative by flow cytometric analysis. With the use of an IntraStain kit (Becton Drive Biosciences), intracellular H-PGDS was detected by staining with polyclonal rabbit antihuman H-PGDS antibody (dilution 1:50, Cayman Biochemical) followed by antirabbit Alexa Fluor 647 (dilution 1:200, Life Technologies, Tokyo, Japan). The expression of H-PGDS was analyzed for mean fluorescence intensity.

For purification of eosinophils, the peripheral blood of patients with mild allergic rhinitis was collected by negative selection by using Eosinophil Isolation Kit (Miltenyl Biotec, Bergisch Gladbach, Germany). Both the purity and the viability of eosinophils were confirmed to exceed 95%.

Cell culture

Normal human epidermal keratinocytes (Kurabo, Osaka, Japan) were grown in Humedia-KG2 medium (Kurabo) with human epidermal growth factor (0.1 ng/mL), insulin (10 μg/mL), hydrocortisone (0.5 μg/mL), gentamicin (50 μg/mL), amphotericin B (50 ng/mL), and bovine brain pituitary extract (0.4%, v/v). Primary skin fibroblasts were isolated by standard methods[23] from healthy human skin and were cultured grown in Dulbecco modified Eagle medium (Gibco, Karlsrude, Germany) with 10% FBS (Gibco).

The immortalized human sebaceous gland cell lines SZ95 (a kind gift from Dr Christos C. Zouboulis) were cultured in sebomed basal medium (Biochrom AG, Berlin, Germany) with 10% FBS and recombinant human epidermal growth factor (Sigma Chemical, St Louis, Mo).

As for normal human epidermal keratinocytes and fibroblasts, the cells grew to 80% to 90% confluent and were starved for 3 hours, followed by treatment with PGD_2 (10 μM) (Cayman Biochemical) for 24 hours at 37°C in 5% CO_2.

Agonists used were the DP agonist BW245c (Cayman Biochemical), the chemoattractant–homologous receptor expressed on T_H2 cells (CRT_H2) agonist 15-keto-PGD_2 (DK-PGD_2) (Cayman Biochemical), and the PPARγ agonist 15-deoxy-Δ 12,14-PGJ_2 (15d-PGJ_2) (Cayman Biochemical). Antagonists used were the DP antagonist BWA868c (Cayman Biochemical), the CRT_H2 antagonist CAY10471 (Cayman Biochemical), and the PPARγ antagonist GW9662 (Cayman Biochemical). Sebocytes were starved for 3 hours and treated with PGD_2 (1-20 μM), BW245c (1-10 μM), DK-PGD_2 (1-10 μM), and 15d-PGJ_2 (1-7 μM) for 21 hours at the confluency of 30% to 40%. For treatment with antagonists, BWA868c (1-10 μM), CAY10471 (1-10 μM), and GW9662 (1-3 μM) (Cayman Biochemical) were preadded at 30 minutes.

SZ95 cells were transfected with PPARγ small-interfering RNA (siRNA) or nontargeting siRNA (Dharmacon, Lafayette, Colo) at 20% confluence by using Lipofectamine 2000 (Life Technologies). At 48 hours after transfection, the cells were starved for 3 hours and treated with or without PGD_2 (7.5 μM) for an additional 21 hours.

For detection of PGD_2, purified eosinophils (1×10^6 cells per well) were incubated in 50 μL of RPMI 1640 with 10% FBS in the presence and absence of 10^{-6} mol/L phorbol 12-myristate 13-acetate (Sigma-Aldrich, St Louis, Mo) and 10^{-5} mol/L calcium ionophore A23187 (Sigma-Aldrich). The concentration of PGD_2 in the supernatant was detected by the use of PGD_2-MOX Enzyme Immunoassay Kit (Cayman Biochemical).

Quantitative RT-PCR

Total RNA was isolated with RNeasy kits and digested with DNase I (Qiagen, Hilden, Germany). The cDNA was reverse transcribed from total RNA samples by using the Prime Script RT reagent kit (Takara Bio, Otsu, Japan). Quantitative RT-PCR was performed by using Light Cycler 480 SYBR Green I Master (Roche, Mannheim, Germany) and the Light Cycler real-time PCR apparatus (Roche) according to the manufacturer's instructions. The primers used for PCR had the following sequences: eotaxin-1, 5′-CTC CGCAGCACTTCTGTGGC-3′ (forward) and 5′- GGTCGGCACAGA-TATCCTTG-3′ (reverse); eotaxin-2, 5′-GCCTTCTGTTCCTGGGTGTC-3′ (forward) and 5′- CCTCCTGAGTCTCCACCTTG-3′ (reverse); eotaxin-3, 5′-CCTCCTGAGTCTCCACCTTG-3′ (forward) and 5′-AAGGGGCTTGT

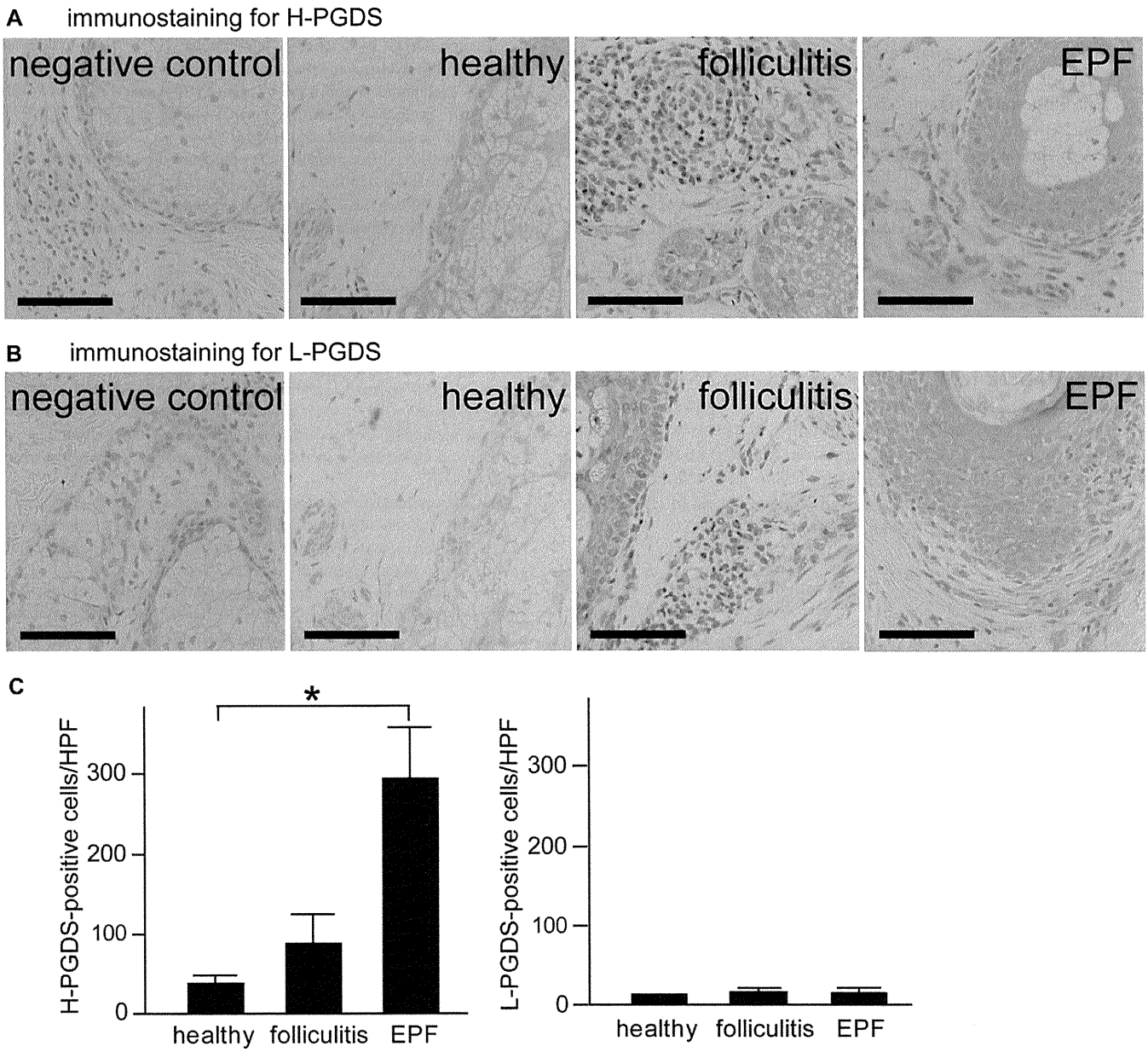

FIG 1. Immunohistochemistry of PGDS. Skin specimens taken from healthy subjects (n = 4), patients with folliculitis (n = 6), and patients with EPF (n = 5) were immunostained for H-PGDS **(A)** and L-PGDS **(B)** and respective negative controls. The infiltrating inflammatory cells around the pilosebaceous gland in EPF were stained with anti–H-PGDS antibody. **C,** The numbers of H-PGDS– and L-PGDS–positive cells were counted. Bar = 100 μm. *$P < .05$. *HPF,* High power field.

GGCTGTATT-3′ (reverse); PPARγ, 5′-ACAGACAAATCACCATTCGT-3′ (forward) and 5′-CTCTTTGCTCTGCTCCTG-3′ (reverse); and Glyceraldehyde 3-phospate dehydrogenase (GAPDH), 5′-AATGTCACCGTTGTC CAGTTG-3′ (forward) and 5′- GTGGCTGGGGCTCTACTTC-3′ (reverse). The results were normalized to those of the housekeeping GAPDH mRNA.

Statistical analysis

Unless otherwise indicated, data are presented as means ± SD and are a representative of 3 independent experiments. *P* values were calculated with the 2-tailed Student *t* test. *P* values less than .05 are considered to be significantly different between the indicated groups and are shown as asterisk in the figures.

RESULTS

Increased H-PGDS expression in EPF lesions

To verify PGDS expression in EPF lesions, we performed immunostaining with anti–H-PGDS and anti–L-PGDS antibodies. We found that the infiltrating inflammatory cells around pilosebaceous units were strongly positive for H-PGDS in lesions from patients with EPF, but not in healthy subjects (Fig 1, *A*). There were a few cells stained for L-PGDS (Fig 1, *B*). The number of H-PGDS–positive cells was significantly greater in EPF skin lesions than in normal healthy skin samples or in folliculitis lesions (Fig 1, *C*).

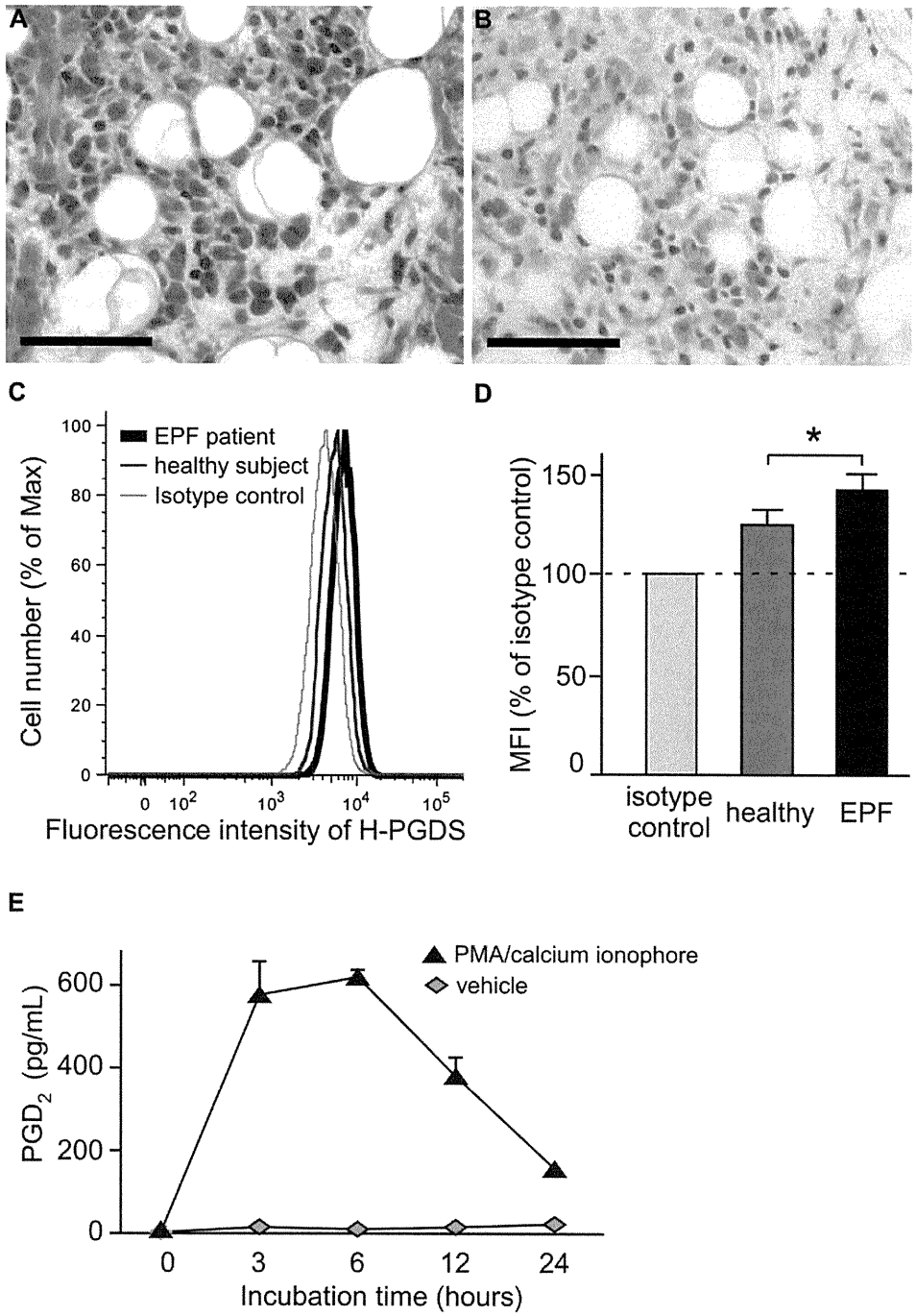

FIG 2. H-PGDS expression and PGD_2 production in eosinophils. Skin specimens of patients with EPF were stained with hematoxylin-eosin **(A)** and anti–H-PGDS antibody **(B)**. Bar = 100 μm. H-PGDS expression in eosinophils was determined by flow cytometry. **C,** Representative flow cytometry results. **D,** The MFI of isotype control was set as 100%, and the MFI of H-PGDS was calculated accordingly (n = 3). *$P < .05$. **E,** PGD_2 levels in eosinophil culture supernatants with or without phorbol 12-myristate 13-acetate and calcium ionophore. *MFI,* Mean fluorescence intensity.

H-PGDS expression and PGD_2 production in eosinophils

Numerous infiltrating eosinophils were stained with anti–H-PGDS antibody (Fig 2, *A* and *B*), suggesting that eosinophils may express H-PGDS. In fact, flow cytometric analysis showed that H-PGDS was detected in eosinophils, and its expression level was higher in patients with EPF than in healthy subjects (Fig 2, *C* and *D*). In addition, we examined the production of PGD_2 from the supernatant of eosinophil culture at 0, 3, 6, 12, and 24 hours after incubation with or without phorbol 12-myristate 13-acetate and calcium ionophore. We found that a significant amount of PGD_2 was produced by eosinophils activated with phorbol 12-myristate 13-acetate and calcium ionophore (Fig 2, *E*).

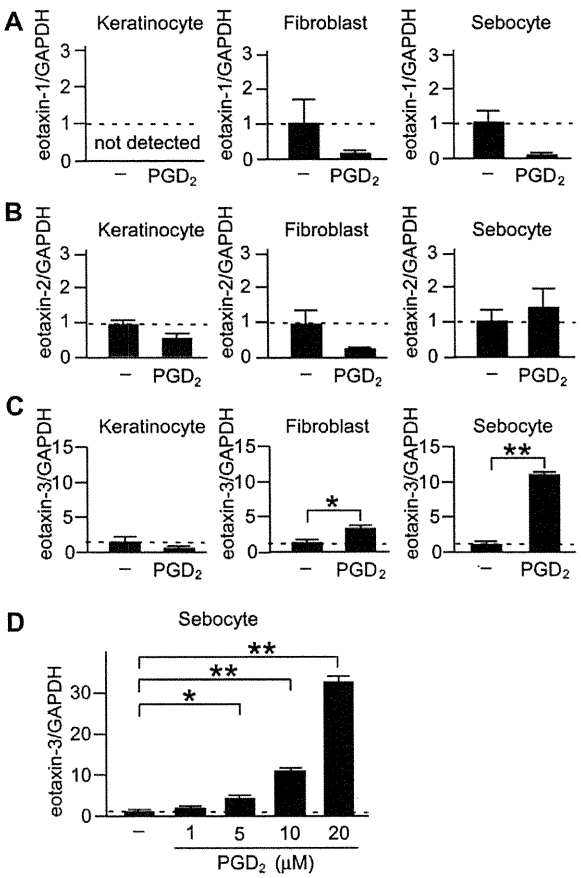

FIG 3. Effect of PGD_2 on eotaxin mRNA expression in human keratinocytes, fibroblasts, and the sebaceous gland cell line SZ95. Cells were incubated with PGD_2 (**A-C**; 10 μM). The mRNA expression levels of eotaxin-1 (Fig 3, *A*), eotaxin-2 (Fig 3, *B*), and eotaxin-3 (Fig 3, *C* and *D*) were evaluated by means of quantitative RT-PCR and normalized according to that of GAPDH. Data are shown as arbitrary units where the value for an unstimulated sample is set at 1 (n = 4). $*P < .05$, $**P < .01$.

PGD_2 increased eotaxin-3 mRNA expression in human sebocytes

We next asked whether PGD_2 could affect the production of chemokines for eosinophil migration. Since the diagnostic hallmark of EPF is the accumulation of eosinophils around the pilosebaceous units, we focused on sebocytes, the cells that constitute the pilosebaceous glands, as well as on keratinocytes and fibroblasts. We found that PGD_2 did not affect the expression of eotaxin-1 or -2 in human keratinocytes, fibroblasts, or sebocytes (Fig 3, *A* and *B*). It did induce eotaxin-3 expression, only slightly in fibroblasts but markedly in the human sebaceous gland cell line SZ95 (Fig 3, *C*). Moreover, we observed that PGD_2 increased eotaxin-3 mRNA expression in sebocytes in a dose-dependent manner (Fig 3, *D*). These findings suggest that PGD_2 induces eotaxin-3 production abundantly in sebocytes and that sebocytes might play a key role in eosinophil trafficking to the pilosebaceous units in EPF.

Dispensable role of the DP1 and CRT_H2 receptors in PGD_2-induced eotaxin-3 expression

Two receptors for PGD_2 have been identified: one is DP1, and the other is CRTH2, also known as DP2, both of which are G protein–coupled receptors.[24,25] We next undertook to determine which receptor mediates eotaxin-3 upregulation by PGD_2. Neither the DP1 agonist BW245c nor the CRT_H2 agonist DK-PGD_2 induced eotaxin-3 in the human sebaceous gland cell lines SZ95 (Fig 4, *A*). In addition, eotaxin-3 upregulation induced by PGD_2 was not suppressed by either the DP1 antagonist BW868c or the CRT_H2 antagonist CAY10471 (Fig 4, *B*).

Involvement of PPARγ in PGD_2-induced eotaxin-3 expression in human sebocytes

PGD_2 spontaneously converts into the cyclopentenone PGs of the J series, such as PGJ_2, $\Delta 12$-PGJ_2,[12] and 15d-PGJ_2.[26] We found that 15d-PGJ_2 dose dependently increased eotaxin-3 expression in sebocytes (Fig 5, *A*). PGJ_2 elicits its function through PPARγ, and the PPARγ antagonist GW9662 suppressed 15d-PGJ_2–induced eotaxin-3 increase in a dose-dependent manner (Fig 5, *B*). We also observed that PGD_2-induced eotaxin-3 increase was suppressed by GW9662 in a dose-dependent manner (Fig 5, *C*). In addition, we examined the effect of PPARγ knockdown by RNA interference in order to confirm the role of PPARγ in PGD_2-induced eotaxin-3 expression. We observed that PPARγ mRNA expression was inhibited by PPARγ siRNA and that PGD2-induced eotaxin-3 increase in sebocytes was suppressed by siRNA knockdown of PPARγ (Fig 5, *D*). In addition, we compared PPARγ expression among keratinocytes, fibroblasts, and sebocytes and found that it was higher in sebocytes than in keratinocytes and fibroblasts (Fig 5, *E*). These data suggest that PGD_2 induces eotaxin-3 expression in sebocytes, through PPARγ, which is highly expressed in sebocytes. Consistently, eotaxin-3 expression tended to be greater in sebocytes of EPF lesions than in those of normal skin samples (Fig 5, *F*).

DISCUSSION

In our current study, H-PGDS was detected in eosinophils by means of flow cytometric analysis, and these H-PGDS–positive cells were accumulated around the pilosebaceous areas in EPF, implying that PGD_2 is abundantly produced in this condition. In addition, eotaxin-3, which is produced by sebocytes via PPARγ upon stimulation by PGD_2, was highly expressed in the sebaceous glands in EPF lesions, likewise implying an abundance of PGD_2 in EPF. These findings may provide an explanation of the massive eosinophil infiltration that occurs around the pilosebaceous units in EPF.

Since indomethacin is generally effective against EPF, COX metabolites are presumed to be involved in the pathomechanism of EPF. Among these COX metabolites, the prostanoid PGD_2 has previously been reported to directly attract inflammatory cells such as T_H2 cells, eosinophils, and basophils and to be involved in chronic allergic inflammation.[17,27] This partly explains how the prostanoids are involved in the mechanism of EPF. Yet it remains unclear how eosinophils infiltrate the pilosebaceous units. In this study, we found that PGD_2 induces eotaxin-3 upregulation in sebocytes. PGD_2 enhances eotaxin-3 expression even in fibroblasts. Since the dermal papilla is a discrete population of specialized fibroblasts, PGD_2 may indirectly attract eosinophils via eotaxin produced by sebocytes and dermal papilla cells.

The underlying mechanism of controlling EPF by indomethacin has been reported to be attributed to the downregulation of CRT_H2 expression.[28] This is an intriguing observation; however,

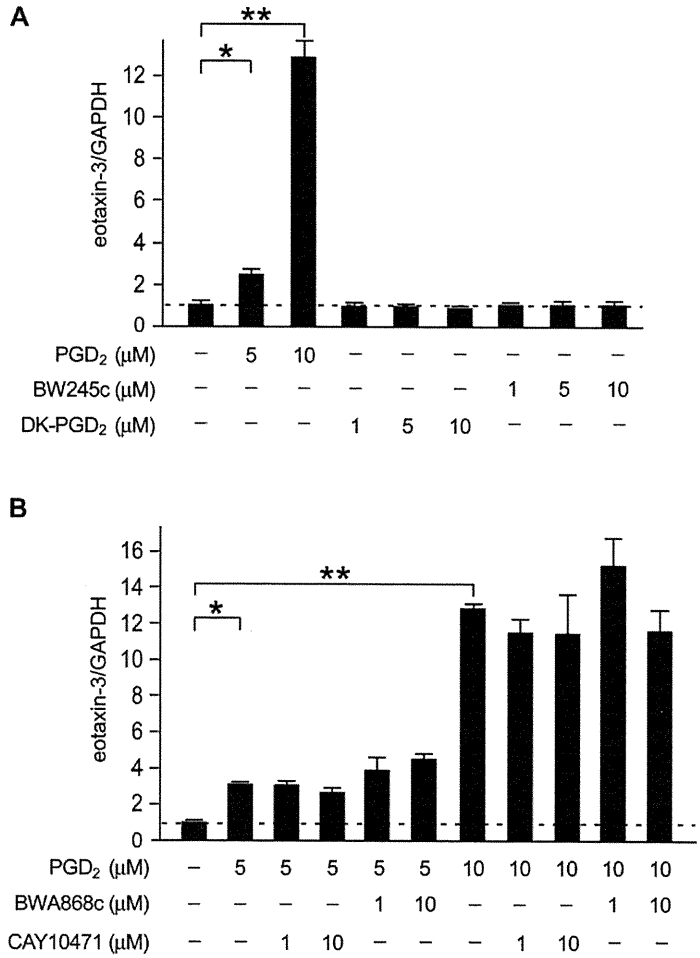

FIG 4. Role of DP1 and CRT_H2 in eotaxin-3 mRNA expression in human sebocytes. SZ95 cells were incubated with PGD_2 in the presence or absence of the DP1 agonist BW245c and the CRT_H2 agonist DK-PGD_2 **(A)** or the DP1 antagonist BW868c and the CRT_H2 antagonist CAY10471 **(B)**. Eotaxin mRNA levels were evaluated by quantitative RT-PCR, and data are shown as arbitrary units where the value for an unstimulated sample is set at 1 (n = 4). $*P < .05$, $**P < .01$.

it remains unclear how indomethacin is specifically effective against EPF. Only a few reports have addressed the efficacy of indomethacin on the other eosinophil-infiltrating skin disorders.[29,30] Our findings indicate that H-PGDS is expressed in peripheral eosinophils of patients with EPF, whereas it is only marginally expressed in those of healthy subjects; nevertheless, it remains uncertain how this difference between patients with EPF and healthy subjects arises. This unique expression profile of H-PGDS in EPF may explain the initiation and/or maintenance of the disease. H-PGDS expression is evident in T cells, and it has recently been reported that CCR8+ T_H2 cells are essential to attract eosinophils to the skin.[31] We detected some T-cell infiltration around the pilosebaceous units in EPF (data not shown), suggesting that CCR8+ T cells and eosinophils jointly initiate and maintain eosinophil infiltration into EPF skin lesions.

It has been demonstrated that sebocytes are capable of producing the neutrophil chemoattractant CXCL8, which may play a role in the pathogenesis of acne,[32] but it remains unknown whether and how sebocytes produce eosinophil chemoattractants. Here we have demonstrated for the first time that eotaxin-3 mRNA expression in sebocytes was enhanced by incubation with PGD_2 and 15d-PGJ_2 and mediated by PPARγ but not by DP1 or CRT_H2. It has been reported that 15d-PGJ_2 binds to PPARγ where it promotes adipocyte differentiation[33,34] and that PPARγ is detected in sebocytes where it is involved in lipid synthesis.[35-37] In our study, larger quantities of PPARγ were detected in sebocytes than in keratinocytes or fibroblasts. Therefore, sebocytes may play an important role in attracting eosinophils into the skin under certain conditions.

Conclusions

We found that H-PGDS is expressed in EPF lesions and that PGD_2 and its metabolite 15d-PGJ_2 induce marked upregulation of eotaxin-3 via PPARγ in sebocytes. These results may explain how EPF shows a massive eosinophil infiltration around pilosebaceous units.

Clinical implications: Inhibition of the PGD_2/PGJ_2-PPARγ pathway may be a therapeutic target for EPF and other diseases involving eosinophil infiltration.

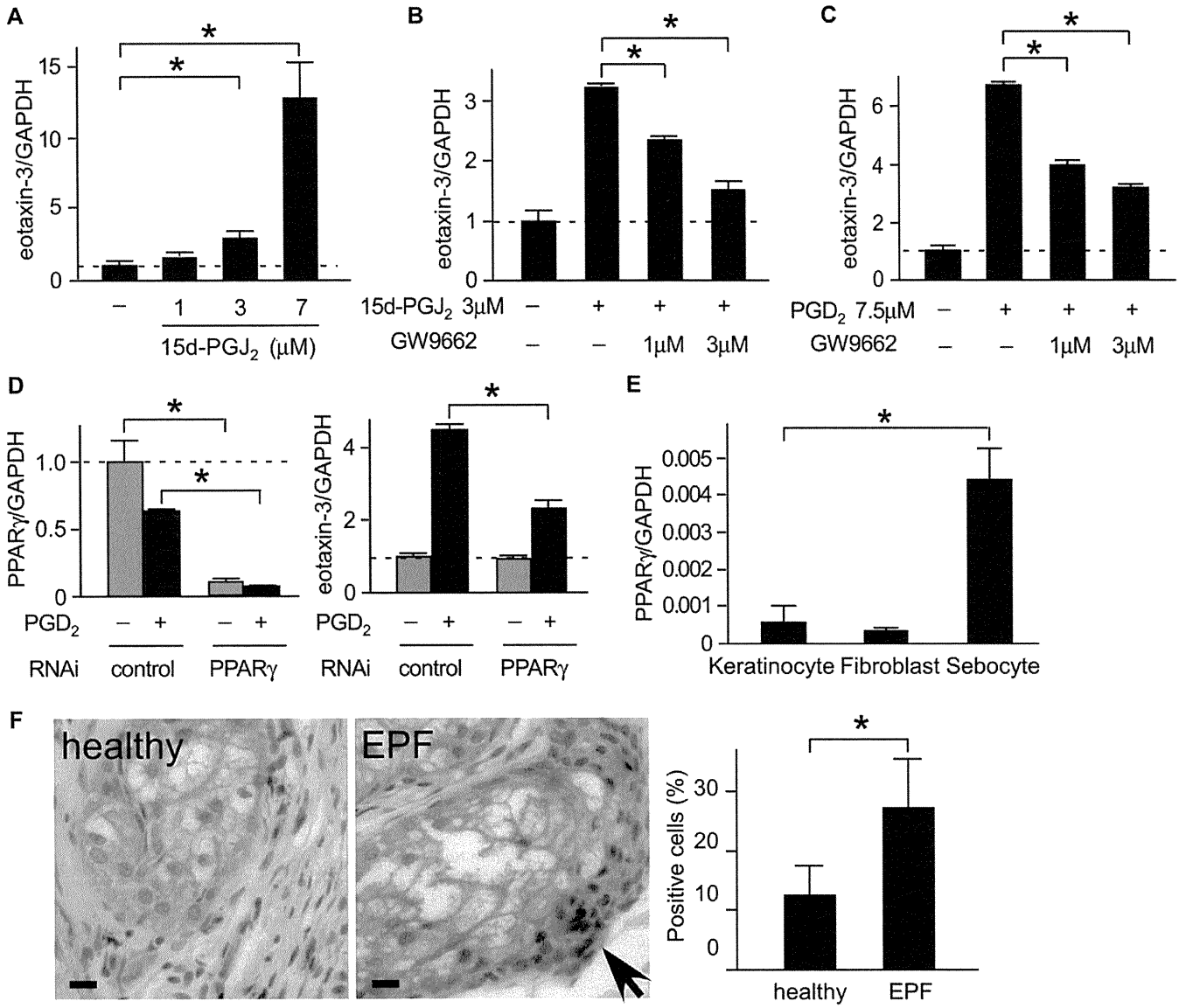

FIG 5. Involvement of PPARγ in eotaxin-3 mRNA expression in sebocytes. SZ95 cells were incubated with 15d-PGJ_2 **(A** and **B)** or PGD_2 **(C)** in the presence or absence of the PPARγ antagonist GW9662 *(Fig 5, B* and *C).* Eotaxin mRNA levels were evaluated by means of quantitative RT-PCR. **D,** The effect of transfection with PPARγ siRNA on mRNA expressions for PPARγ and eotaxin-3. **E,** PPARγ mRNA expression in normal human epidermal keratinocytes, fibroblasts, and SZ95 cells. **F,** Immunostaining for eotaxin-3. Sebocytes strongly positive for eotaxin-3 are indicated by an arrow (right panel). The percentage positive for eotaxin-3 among sebocytes was examined (n = 3 each, right panel). Bar = 10 μm. $*P < .05$.

REFERENCES

1. Ofuji S, Furukawa F, Miyachi Y, Ohno S. Papuloerythroderma. Dermatologica 1984;169:125-30.
2. Kabashima K, Sakurai T, Miyachi Y. Treatment of eosinophilic pustular folliculitis (Ofuji's disease) with tacrolimus ointment. Br J Dermatol 2004;151:949-50.
3. Sugita K, Kabashima K, Koga C, Tokura Y. Eosinophilic pustular folliculitis successfully treated with sequential therapy of interferon-gamma and ciclosporin. Clin Exp Dermatol 2006;31:709-10.
4. Lankerani L, Thompson R. Eosinophilic pustular folliculitis: case report and review of the literature. Cutis 2010;86:190-4.
5. Teraki Y, Konohana I, Shiohara T, Nagashima M, Nishikawa T. Eosinophilic pustular folliculitis (Ofuji's disease): immunohistochemical analysis. Arch Dermatol 1993;129:1015-9.
6. Fushimi M, Tokura Y, Sachi Y, Hashizume H, Sudo H, Wakita H, et al. Eosinophilic pustular folliculitis effectively treated with recombinant interferon-gamma: suppression of mRNA expression of interleukin 5 in peripheral blood mononuclear cells. Br J Dermatol 1996;134:766-72.
7. Sano S, Itami S, Azukizawa H, Araki Y, Higashiyama M, Yoshikawa K. Interleukin 5-inducing activity in the blister fluid of eosinophilic pustular dermatosis. Br J Dermatol 1999;141:154-5.
8. Rankin SM, Conroy DM, Williams TJ. Eotaxin and eosinophil recruitment: implications for human disease. Mol Med Today 2000;6:20-7.
9. Amerio P, Frezzolini A, Feliciani C, Verdolini R, Teofoli P, De Pita O, et al. Eotaxins and CCR3 receptor in inflammatory and allergic skin diseases: therapeutical implications. Curr Drug Targets Inflamm Allergy 2003;2:81-94.
10. Dulkys Y, Schramm G, Kimmig D, Knoss S, Weyergraf A, Kapp A, et al. Detection of mRNA for eotaxin-2 and eotaxin-3 in human dermal fibroblasts and their distinct activation profile on human eosinophils. J Invest Dermatol 2001;116:498-505.
11. Kagami S, Saeki H, Komine M, Kakinuma T, Tsunemi Y, Nakamura K, et al. Interleukin-4 and interleukin-13 enhance CCL26 production in a human keratinocyte cell line, HaCaT cells. Clin Exp Immunol 2005;141:459-66.
12. Fukamachi S, Kabashima K, Sugita K, Kobayashi M, Tokura Y. Therapeutic effectiveness of various treatments for eosinophilic pustular folliculitis. Acta Derm Venereol 2009;89:155-9.

13. Narumiya S, Sugimoto Y, Ushikubi F. Prostanoid receptors: structures, properties, and functions. Physiol Rev 1999;79:1193-226.
14. Kabashima K, Miyachi Y. Prostanoids in the cutaneous immune response. J Dermatol Sci 2004;34:177-84.
15. Honda T, Tokura Y, Miyachi Y, Kabashima K. Prostanoid receptors as possible targets for anti-allergic drugs: recent advances in prostanoids on allergy and immunology. Curr Drug Targets 2010;11:1605-13.
16. Sturm EM, Schratl P, Schuligoi R, Konya V, Sturm GJ, Lippe IT, et al. Prostaglandin E2 inhibits eosinophil trafficking through E-prostanoid 2 receptors. J Immunol 2008;181:7273-83.
17. Hirai H, Tanaka K, Yoshie O, Ogawa K, Kenmotsu K, Takamori Y, et al. Prostaglandin D2 selectively induces chemotaxis in T helper type 2 cells, eosinophils, and basophils via seven-transmembrane receptor CRTH2. J Exp Med 2001;193: 255-61.
18. Urade Y, Eguchi N. Lipocalin-type and hematopoietic prostaglandin D synthases as a novel example of functional convergence. Prostaglandins Other Lipid Mediat 2002;68-69:375-82.
19. Takeda K, Yokoyama S, Aburatani H, Masuda T, Han F, Yoshizawa M, et al. Lipocalin-type prostaglandin D synthase as a melanocyte marker regulated by MITF. Biochem Biophys Res Commun 2006;339:1098-106.
20. Urade Y, Ujihara M, Horiguchi Y, Igarashi M, Nagata A, Ikai K, et al. Mast cells contain spleen-type prostaglandin D synthetase. J Biol Chem 1990;265:371-5.
21. Kanaoka Y, Urade Y. Hematopoietic prostaglandin D synthase. Prostaglandins Leukot Essent Fatty Acids 2003;69:163-7.
22. Shimura C, Satoh T, Igawa K, Aritake K, Urade Y, Nakamura M, et al. Dendritic cells express hematopoietic prostaglandin D synthase and function as a source of prostaglandin D2 in the skin. Am J Pathol 2011;176:227-37.
23. Ham RG. Dermal fibroblasts. Methods Cell Biol 1980;21A:255-76.
24. Boie Y, Sawyer N, Slipetz DM, Metters KM, Abramovitz M. Molecular cloning and characterization of the human prostanoid DP receptor. J Biol Chem 1995; 270:18910-6.
25. Nagata K, Hirai H. The second PGD(2) receptor CRTH2: structure, properties, and functions in leukocytes. Prostaglandins Leukot Essent Fatty Acids 2003;69:169-77.
26. Shibata T, Kondo M, Osawa T, Shibata N, Kobayashi M, Uchida K. 15-Deoxy-delta 12,14-prostaglandin J2: a prostaglandin D2 metabolite generated during inflammatory processes. J Biol Chem 2002;277:10459-66.
27. Monneret G, Gravel S, Diamond M, Rokach J, Powell WS. Prostaglandin D2 is a potent chemoattractant for human eosinophils that acts via a novel DP receptor. Blood 2001;98:1942-8.
28. Satoh T, Shimura C, Miyagishi C, Yokozeki H. Indomethacin-induced reduction in CRTH2 in eosinophilic pustular folliculitis (Ofuji's disease): a proposed mechanism of action. Acta Derm Venereol 2010;90:18-22.
29. Fallah H, Dunlop K, Kossard S. Successful treatment of recalcitrant necrotizing eosinophilic folliculitis using indomethacin and cephalexin. Australas J Dermatol 2006;47:281-5.
30. Tanglertsampan C, Tantikun N, Noppakun N, Pinyopornpanit V. Indomethacin for recurrent cutaneous necrotizing eosinophilic vasculitis. J Med Assoc Thai 2007;90: 1180-2.
31. Islam SA, Chang DS, Colvin RA, Byrne MH, McCully ML, Moser B, et al. Mouse CCL8, a CCR8 agonist, promotes atopic dermatitis by recruiting IL-5+ T(H)2 cells. Nat Immunol 2011;12:167-77.
32. Nagy I, Pivarcsi A, Kis K, Koreck A, Bodai L, McDowell A, et al. Propionibacterium acnes and lipopolysaccharide induce the expression of antimicrobial peptides and proinflammatory cytokines/chemokines in human sebocytes. Microbes Infect 2006;8:2195-205.
33. Forman BM, Tontonoz P, Chen J, Brun RP, Spiegelman BM, Evans RM. 15-Deoxy-delta 12, 14-prostaglandin J2 is a ligand for the adipocyte determination factor PPAR gamma. Cell 1995;83:803-12.
34. Kliewer SA, Lenhard JM, Willson TM, Patel I, Morris DC, Lehmann JM. A prostaglandin J2 metabolite binds peroxisome proliferator-activated receptor gamma and promotes adipocyte differentiation. Cell 1995;83:813-9.
35. Chen W, Yang CC, Sheu HM, Seltmann H, Zouboulis CC. Expression of peroxisome proliferator-activated receptor and CCAAT/enhancer binding protein transcription factors in cultured human sebocytes. J Invest Dermatol 2003;121: 441-7.
36. Alestas T, Ganceviciene R, Fimmel S, Muller-Decker K, Zouboulis CC. Enzymes involved in the biosynthesis of leukotriene B4 and prostaglandin E2 are active in sebaceous glands. J Mol Med 2006;84:75-87.
37. Makrantonaki E, Zouboulis CC. Testosterone metabolism to 5-alpha-dihydrotestosterone and synthesis of sebaceous lipids is regulated by the peroxisome proliferator-activated receptor ligand linoleic acid in human sebocytes. Br J Dermatol 2007;156:428-32.

パッチテストアレルゲンに関するアンケート2010

鈴木加余子，松永佳世子

日本皮膚アレルギー・接触皮膚炎学会雑誌
Journal of Environmental Dermatology and Cutaneous Allergology

Vol. 5 No.2 (Serial No. 20) : 91-102, 2011

J Environ Dermatol Cutan Allergol. 5 (2) : 91-102, 2011

研　究

パッチテストアレルゲンに関するアンケート2010

鈴木加余子[1)]，松永佳世子[2)]

要　旨

現在国内で保険収載され販売されているパッチテストアレルゲンは鳥居薬品の40種と佐藤製薬の6種しかなく，われわれ皮膚科医は多くのパッチテストアレルゲンを海外から個人購入している。また，パッチテストの保険点数は低く，パッチテストを施行すると赤字となる。

このような現状を踏まえて，日本皮膚アレルギー・接触皮膚炎学会の個人会員を対象としたパッチテストに関するアンケートを2010年2月に施行した。その結果，回答した医師の9割以上が接触皮膚炎の原因追求においてパッチテストは必要と感じているが，その実施状況は「よく実施している」が29%，「時々実施している」が62%という結果であった。パッチテストを施行しない医師は9%で，その主な理由は，「手間がかかる」，「アレルゲンの入手が困難」ということであった。パッチテストの実施状況については，97%が日本ではパッチテストが充分に実施されていないと感じており，その理由として，90%が国内で販売されているパッチテストの種類が少ないことを挙げた。

また，84%が保険診療におけるパッチテストには問題があると回答し，具体的には保険点数が低いことが問題点として上がった。TRUE Testについては，使用経験のない医師が98%を占めたが，82%はこのようなready to useのパッチテストアレルゲン製品により今後パッチテスト症例が増えると感じていた。

(J Environ Dermatol Cutan Allergol. 5 (2) : 91-102, 2011)

キーワード：パッチテスト，アレルゲン，保険点数，アンケート

はじめに

接触皮膚炎はその原因を明らかにして，原因物質との接触を避ければ根治できる疾患であり，パッチテストは接触皮膚炎の原因を検出するために必要かつ最も有用な検査方法である。

しかしながら，これまで日本国内で保険収載され販売されているパッチテスト用アレルゲンは鳥居薬品の40品目（Table 1，金属17種，その他23種）しかなく，われわれはジャパニーズスタンダードアレルゲンも含めて，診断に必要なアレルゲンの多くを海外から個人購入している。アレルゲン購入手順が煩雑であることやパッチテストの準備に人手を要すること，アレルゲン購入費用や人件費に比較してパッチテストの保険点数が極端に低いことから，皮膚科医でもパッチテストを積極的に行っていない現状がある。

2009年9月にready-to-useとなっているパッチテスト用アレルゲン（Table 1，商品名：パッチテストテープ[1)]，佐藤製薬）6種が保険承認されたことを契機に本学会員を対象としてパッチテストアレルゲンについてのアンケート調査を実施したのでその結果を報告する。

＜アンケート＞

目的：

①パッチテストの実施状況の把握

②パッチテストアレルゲン試薬の入手状況と入手

[1)] 刈谷豊田総合病院皮膚科
〒448-8505　刈谷市住吉町5-15
[2)] 藤田保健衛生大学医学部皮膚科学
連絡先：鈴木加余子

掲載決定日：2011年2月14日